The University of South Bohemia in České Budějovice
Faculty of Science

Species identification and phylogenetic comparative analyses of butterfly wing phenotypes in a tropical locality

Bachelor thesis

Chau Doan Tran

Supervisor: RNDr. Pável Matos-Maraví, Ph.D., Biology Centre, CAS

Consultant: MSc. Daniel Linke, Faculty of Sciences, Department of Zoology

České Budějovice 2023

BIBLIOGRAPHICAL DETAIL

Chau T., 2023: Species identification and phylogenetic comparative analyses of butterfly wing phenotypes in a tropical locality. Bc. Thesis, in English. – 49 p., Faculty of Science, University of South Bohemia, České Budějovice, Czech Republic.

ANNOTATION

The goal of this research is to investigate whether butterfly morphometrics (phenotypic traits) are reliable predictors of the thermal buffering ability of butterflies from a tropical community in the Andean foothills. Results are discussed in the context of published information in biological, ecological, and bioinformatics articles.

DECLARATION

I declare that I am the author of this qualification thesis and that in writing it I have used the sources and literature displayed in the list of used sources only.

Place, Date

Signature

ACKNOWLEDGEMENTS

ABSTRACT

The thermal buffering ability of ectotherms describes how their body temperatures are adjusted under varying ambient temperatures. Understanding how ectotherms buffer their body temperature is crucial and timely to precisely predict their responses to climate change. The thesis aims to identify the phylogenetic correlations between wing morphometrics (phenotypic traits) and the buffering thermoregulation ability of 71 butterfly species found in the Andean foothills. To do this, we first gather DNA sequences of the COI gene and reconstruct a maximum likelihood phylogeny. Afterwards, we measure the butterfly wing shapes and sizes and compile a dataset consisting of butterfly thorax and ambient temperatures recorded in the field in Peru. Finally, we use phylogenetic comparative methods to find statistical correlations between the butterfly thermal buffering ability predicted by the measured morphological traits: thorax cylindric volume (cm^3), total wing area (cm^2), wing loading (the ratio of thorax volume and total wing area), and aspect ratio (forewing length divided by forewing width). Our results show that butterflies with high aspect ratio, describing species with elongated and narrow wings, have high thermal buffering ability, i.e., they keep stable thorax temperatures across a wide range of ambient temperatures. These butterflies are often associated with long gliding flights, which might reduce heat production by having long non-flapping flight and decreased flight muscle activity. However, other morphometric traits were not associated with butterfly thermal buffering ability, despite previous predictions suggested a correlation between increased body temperatures and increased body sizes together with increased flight speed (assessed by proxy through wing loading). Thermoregulation is important for animals to adapt and survive environmental and climatic change. Our work provides a standardized and replicable approach for forthcoming studies on thermoregulation of butterflies, to assess the thermal buffering ability along environmental gradients in the tropics (e.g., along elevational zones) predicted by ecomorphological traits of ectotherm animals.

Table of Contents

1. Introduction

The climate is changing at an unprecedented pace, affecting ecosystems and species worldwide. In the tropics, the summer days have already been 20% warmer than the average recorded temperatures (Byrne 2021). In 2023, temperatures might break previous records because El Niño is predicted to drive weather and climate extremes worldwide (Rodrigues, 2023). This will likely cause extreme tropical drought and rapid shifts in global mean temperatures. Together with other factors such as extensive deforestation in the tropics, biodiversity will likely face its highest threats ever due to climate extremes.

Species have different strategies to cope with environmental changes, such as tracking of the optimum climate by dispersal or behavioral thermoregulation. However, our understanding of morphological traits predicting effective responses to climate change is limited, especially in species-rich ectotherm groups such as insects, and in biodiverse regions such as the tropics. Climate change and extremes, such as heatwaves, might cause ectothermic animals to become extinct, specially, when they are isolated and cannot relocate via dispersal to a better microclimate (Hayes et al. 2023). Thus, to cope with such conditions, some species including butterflies tend to seek shade and shelters to thermoregulate and lower their body temperature.

1.1. How ectotherms deal with climate change

Ectotherms stand out as a vulnerable group in the context of the ongoing climate crisis, given their dependence on ambient temperatures to regulate their metabolic processes (Johansson, Orizaola, and Nilsson-Örtman 2020). Climate change poses a significant threat to tropical species because they have narrow physiological tolerances to temperature extremes, which might have caused the high estimated frequency of climate-related local extinctions (Grinder and Wiens 2023). Thus, it is timely to understand the potential responses of tropical ectotherm groups to climate change. For example, species might respond to environmental changes by genetic-based adaptations (Kellermann and van Heerwaarden 2019), but ectotherms also employ more often different strategies to thermoregulate, including environmental-driven changes in behavior (Barton, Porter, and Kearney 2014), changes of physiology (Ashe-Jepson et al. 2023), or plastic responses in morphology (Hill et al. 2021).

In terms of physiological tolerances, for example, *Heliconius* butterflies (Nymphalidae) from the Andean foothills have different thermal tolerances along an altitudinal gradient; lowland populations have higher tolerances than high elevation ones (Montejo-Kovacevich et al. 2020). Further, there are phenotypic traits that potentially enhance the thermoregulatory abilities of species, such as dark coloration and body size, which were associated with butterflies occurring in cooler conditions across tropical habitats in Australia (Xing et al. 2016). Regarding behavioral responses to climate changes along microhabitats, Alpine temperate species can utilize warm microclimates, and low-altitude grassland species may seek colder microhabitats to escape heat (Dongmo et al. 2021). However, tropical ectotherms might be more endangered

due to the global warming as they experience temperatures much closer to their physiological optimum than temperate taxa (Johansson, Orizaola, and Nilsson-Örtman 2020). Although, most findings on behavioral thermoregulation reported to date were mostly for temperate ectotherms and butterflies, limited support to similar behaviors in tropical species has been reported. Overall, more research regarding thermoregulatory mechanisms of tropical butterflies, including physiological, ecomorphological, and behavioral responses, is needed to address this gap in knowledge.

1.2. Thermal buffering ability of butterflies in the tropics

Thermal buffering ability is the capacity of an organism to maintain a stable body temperature despite the fluctuations of the ambient temperature (Bladon et al. 2020). Thermoregulation plays an important role in the survival fitness of butterflies.

Buffering ability in butterflies is driven by the interaction of body size, habitat use, and physiological limits (Ashe-Jepson et al. 2023; Kleckova and Klecka 2016). In a community of tropical lowland butterflies, Ashe-Jepson et al. (2023) identified a negative association between thermal buffering ability and physiological thermal tolerance, suggesting a potential trade-off in how butterflies cope with climatic fluctuations and extreme events. Furthermore, smaller species seem to be less efficient in buffering their body temperature (De Keyser et al. 2015), in both temperate (Bladon et al. 2020) and tropical communities (Laird-Hopkins et al. 2023), but they exhibited higher thermal tolerances (Ashe-Jepson et al. 2023). Additionally, wing color and shape seem to be good predictors of butterfly responses to environmental changes. For example, aspect ratio, which is a morphometric measure of how elongated and narrow the forewings are, seem to positively correlate with thermal buffering ability in a community of tropical lowland butterflies (Laird-Hopkins et al. 2023). However, despite these recent efforts to understand the behavioral and phenotypic traits affecting thermal buffering ability, there is still a lack of substantial evidence for other tropical communities and along elevational gradients.

1.3. Work aim

The goal of this research is to investigate whether butterfly morphometrics (phenotypic traits) are reliable predictors of the thermal buffering ability of butterflies from a tropical community in the Andean foothills. In my thesis, we investigate how thermal buffering of butterflies is explained by phylogenetic relatedness of species occurring in the local community, and how thermal buffering is explained by morphological traits. We gather partial DNA sequences of the mitochondrial COI gene and reconstruct the phylogeny of the local butterfly assemblage. We rely on DNA barcoding, which is a method to identify species using a short region of DNA from a specific gene or genes. They are called "barcode" because it uses short, standardized DNA sequences acting as unique identifiers for species. With a molecular phylogeny based on

COI, we then measure wing shapes and sizes of 71 species of the local butterfly assemblage, and compile thorax temperatures recorded in the field in Peru. Our overall aim is to find statistical correlations among thermal buffering ability against morphological traits, such as wing loading, total area (cm^2), aspect ratio and thorax volume (cm^3).

2. Materials and Methods

2.1. Study sites and species

Butterflies were caught at the locality of Tarapoto, which is characterized by a premontane (~400 –800 m) tropical rainforest near a national park (Área de Conservación Regional Cordillera Escalera) in northeastern Peru. The research team (Pável Matos, Daniel Linke, and local collaborators) visited the locality twice, first during the rainy-season of 2021/22 from October to February, and second during the dry-season of 2022 from June to September. The area is covered by ~50-year-old secondary growth forests with small pockets of extensively used farmlands (under 5%). Both climate and flora vary greatly within a very limited geographic scale, influencing the distribution and composition of butterflies in the community. Local conditions ranged from moist and shady valleys, semi-open permaculture plantations, closed secondary forest cut by walking paths to dry, windy hilltops with xerophilic plants.

2.1.1. Data Collection

Butterflies, when encountered during field walking, were captured using entomological nets without active chasing to not bias our records towards artificially increased body temperatures. For data collection, we followed the protocol of Bladon et al. (2020) with minor modifications: Within 5 seconds after capture, the thoracic temperature (T_b) was measured, using a thin thermocouple (0.5 mm diameter) and a handheld thermometer (Tecpel Thermometer 305B, TC Direct); Afterwards, the air temperature was measured in the shade at waist height (T_a). The butterfly was removed from the net and identified to species level, or as taxonomically close as possible, before being either released or collected in glassine envelopes for further analyses. In the present dataset, only the most abundant species/subspecies with at least 10 measured individuals across a range of 16.6 °C to 43.0 °C from T_b and 15.3 °C to 35.2 °C from T_a were used to obtain reliable estimates of per-species thermal buffering ability. Butterfly sampling was random and did not represent true species diversity and composition at the study location.

2.1.2. DNA sequencing

Total DNA was extracted from two butterfly legs per specimen using the QIAGEN's DNeasy kit by a technician. Amplification of the mitochondrial cytochrome c oxidase subunit I (COI) gene was performed using published primers and PCR protocols (Matos-Maraví et al. 2013). DNA sequencing was conducted by the company Macrogen Europe BV (Amsterdam, The Netherlands). The resulting chromatograms and DNA sequences were inspected and edited accordingly using the program Geneious Prime 2023.2.1 (http://www.geneious.com/).

2.2. Phylogenetic Analysis

2.2.1. Bioinformatics pipelines to retrieve BOLD databases.

First, a bioinformatics pipeline was developed to retrieve species sequences from the Barcode of Life Data Systems (BOLD) system, accessible at http://www.boldsystems.org. This retrieval process was facilitated using a command line interface known as "BOLD-CLI," as detailed by Nugent (2019) (Appendix code 1). Subsequently, a series of Bash commands were applied to perform data curation procedures, such as the automatic renaming of sequence headers and removal of DNA sequences that do not come from the COI fragment used for barcoding. Second, local BLAST databases were constructed in the Metacentrum environment (the Czech National Grid Organization, https://metavo.metacentrum.cz/) using the COI sequences retrieved from BOLD (Appendix code 2). Third, we performed BLAST searches using the command '*blastn*' (Altschul et al. 1990) using our samples as queries against the reference database (Appendix code 3). Subsequently, the output data underwent further refinement and filtering procedures using Bash commands, resulting in an Excel file with pairwise sequence identities (P-identity) higher than a threshold of 95%, and highlighting the best high-confidence match per sample as well as the proportion of matches with the same taxonomic name from our local BLAST databases. Altogether, these values were necessary to assess the species identities of our sampled specimens.

2.2.2. COI sequences for missing species

For this study, our focus was a subset of 71 distinct species/subspecies from the field work in Peru because those had robust temperature data to assess thermal buffering ability and photographs to assess morphometrics measures. We were able to sequence and confidently identify 36 species after the BLAST search procedure using our own sequences as queries. Therefore, a total of 35 studied species/subspecies with missing COI sequences were obtained from publicly accessible repositories, specifically the National Center for Biotechnology Information (NCBI) database available at https://www.ncbi.nlm.nih.gov/ supplemented by public data from the BOLD database.

2.2.3. Phylogenetic Tree

To account for the evolutionary relationships among the studied species in the comparative analyses, we inferred a maximum likelihood phylogenetic tree. The obtained COI sequences were aligned using the Multiple Alignment using Fast Fourier Transform (MAFFT) tool v7.520 (Katoh and Standley 2013), which estimated homologous positions along the COI gene (Appendix code 4). To construct the phylogenetic tree using the aligned dataset, we utilized the IQ-TREE multicore software version 2.2.0 (Minh et al. 2020) (Appendix code 5). This allowed us to systematically explore various potential tree topologies and choose the maximum likelihood phylogeny based on our data, with statistical support values estimated using the Ultrafast Bootstrap Approximation (Hoang et al. 2018) with 1,000 replicates. To achieve model accuracy,

we partitioned the COI alignment into codon positions, and allowed the program, via ModelFinder, to find the best partitioning scheme and substitution models using the commands `-m MFP --merge`. Finally, we constrained the relationships among butterfly families and the monophyly for each of them. Ultimately, we assigned the age of the butterfly superfamily (Papilionoidea) to 110 million years, following current estimations (Kawahara et al., 2023).

2.3. Butterfly morphology

Morphology traits were scored based on one photographed specimen per species with a scale reference in millimeters (mm) or centimeters (cm). The photographs were manually retrieved from the online database "Butterflies of America" (https://www.butterfliesofamerica.com/) using the respective species names as search criteria or from the mounted collection in České Budějovice. To ensure reproducibility, all measurements were conducted in accordance with Figure 1. The measurements were executed using the software ImageJ v1.54 software (Schneider, Rasband, and Eliceiri 2012) with the exception of total wing areas, which were measured using the semi-automated MATLAB script "wingImageProcessor 1.1". The aspect ratio was computed by dividing the forewing length by the forewing width.
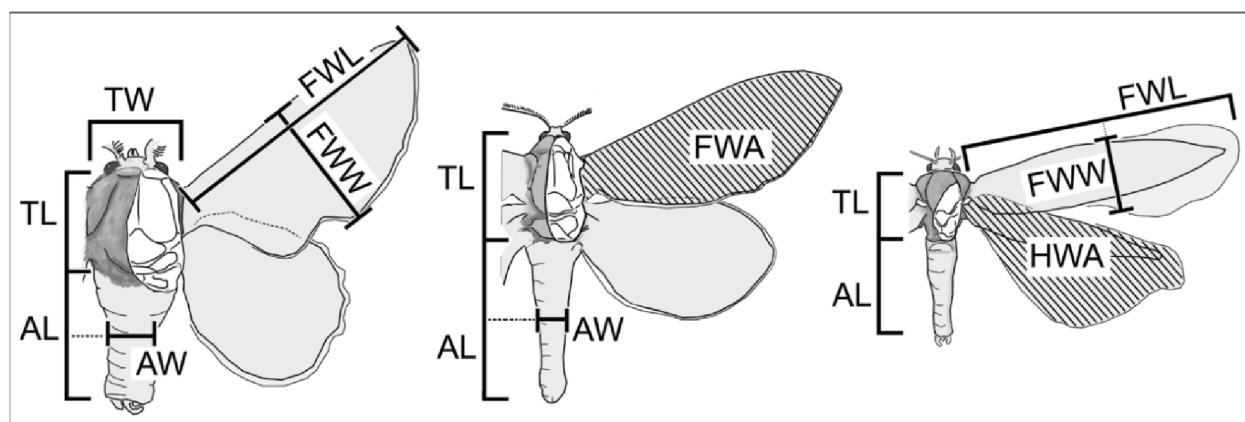
Figure 1. Measurements on the butterfly (García-Barros 2015).

For the total wing area measurements, we first employed Photoshop version 24.1.0 to extract one forewing and one hindwing from images displaying the entire specimen, as depicted in Figure 2. Following this, we imported these wing images into the program wingImageProcessor 1.1. We specified the length of the scale bar in cm and defined a rectangular region of interest, as illustrated in

Figure 3. The program, then, performed automatic calculations of wing area, expressed in square centimeters (cm²). To measure the total wing area for each specimen, we summed the forewing and hindwing areas, and multiplied them by two to account for the four butterfly wings.
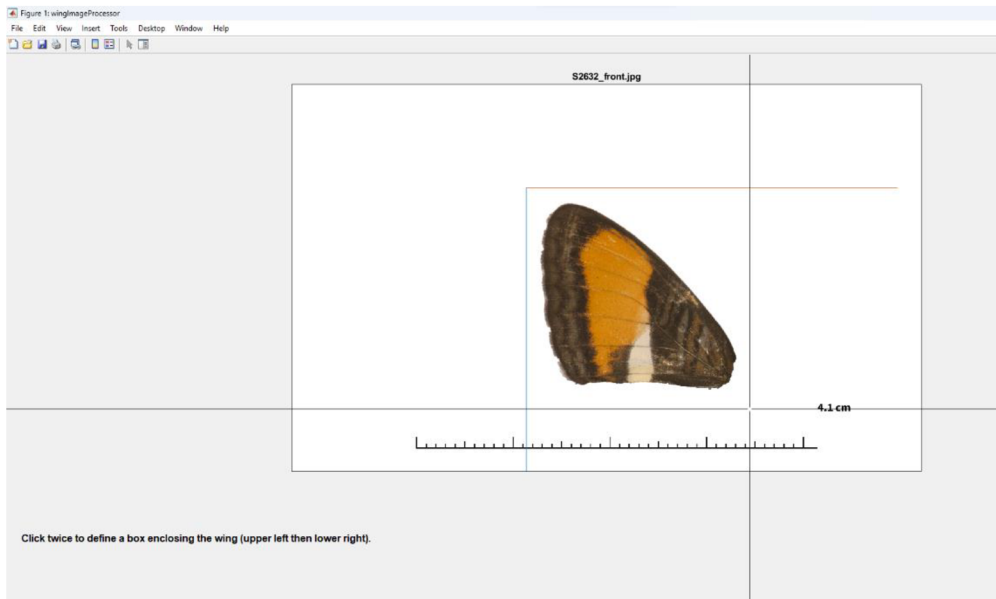
Figure 2. Sampled forewing for analysis in the program wingImageProcessor 1.1.
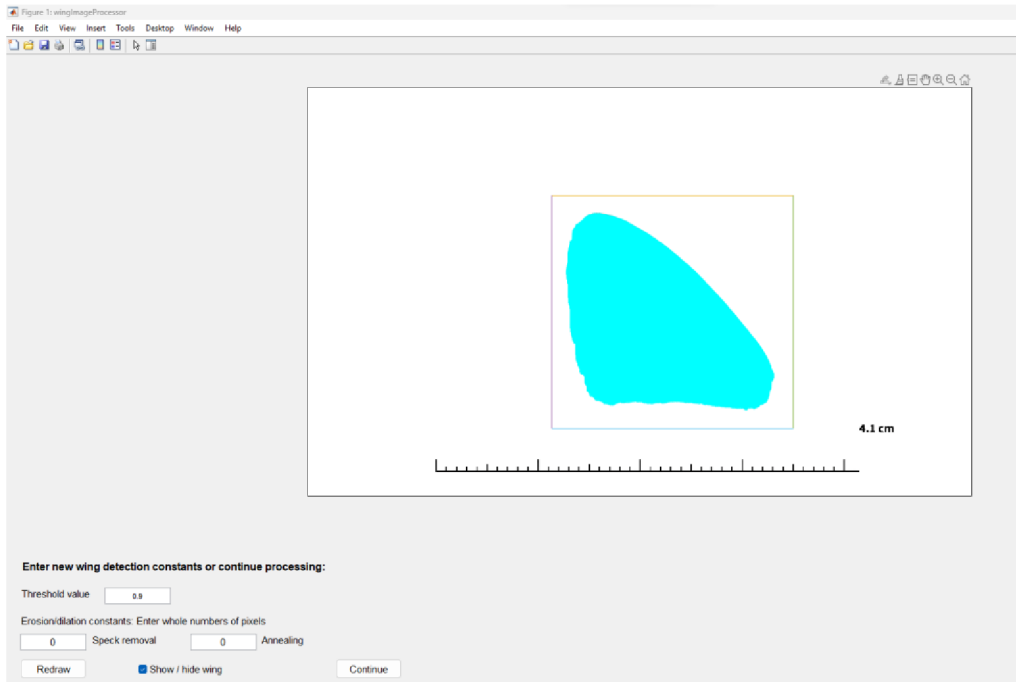
Figure 3. Automated isolation of the region of interest. To isolate the best part of the wing, we used a threshold of 0.9 for all samples, except by minor adjustments for some specimens, while keeping "Speck removal" and "Annealing" parameters at zero.

Wing loading relates the body mass against total wing area. However, our morphometrics measures derive only from photographed individuals, as weight of species was not available. Thus, as a proxy of weight, we used the cylinder volume of thorax, which is the body part harboring the muscles allowing powered flight. We employed the following equation to derive the wing loading:

$$\frac{\left(\pi \times (\frac{TW}{2})^2 \times TL \right)}{TA}$$

Where TW= the thorax width, TL = the thorax length, TA = the total wing area.

2.4. Thermal buffering ability of wild butterflies

We conducted all statistical analyses using R version 4.3.1 (R Core Team 2023).

2.4.1. Thermal buffering ability

We applied a linear regression model to fit the relationship between air temperature (T_a) and butterfly body temperature (T_b) for each studied species/subspecies.We used the command "*lm()*" in R (https://www.rdocumentation.org/packages/stats/versions/3.6.2/topics/lm) to fit the formula *lm*(T_b ~ T_a) (Appendix code 7). This analysis determined the slope of the fitted regression, which served as an indicator of the ability of butterflies to adjust their body temperature in response to variations in ambient temperature (Bladon et al. 2020); the lower the slope of the fitted regression, the higher the thermal buffering ability of the butterfly species (i.e. butterfly keeping stable T_b across a wide range of ambient temperatures).

2.4.2. Associations of buffering ability with morphometrics of butterflies

To test our hypotheses on the effects of butterfly wing morphology in thermal buffering ability, we used two phylogenetic comparative methods, Phylogenetic Independent Contrasts (PIC, Felsenstein 1985a) and Phylogenetic Generalized Least Squares (PGLS, Martins and Hansen 1997) (Appendix code 11). We were interested in whether wing loading, total area, thoracic volume, and aspect ratio, can predict the estimated thermal buffering ability of each studied species. We used the R packages: *nlme* v 3.1.162 (Pinheiro and Bates 2000) for function *gls()* to fit a generalized least squares (GLS) model; *dplyr* v 1.1.3, (Wickham et al. 2023) to manipulate the data; *ape* v 5.7.1 (Paradis and Schliep 2019) for PIC analyses and plotting phylogenetic trees with function *pic()*; *caper* v 1.0.3 (Orme et al. 2023) for PGLS analyses with function *pgls()*. These analytical techniques were implemented under the context of the Brownian motion model of evolution (Felsenstein 1985). Further, to visualize the approximate evolution of each trait along the phylogeny of the 71 studied species, we used the function *contMap()* from the R package *phytools* v 1.9-16 (Revell 2012) to plot the reconstructed ancestral trait states for every internal node reconstructed using the method described in Felsenstein (1985).

3. Results

3.1. Sampled specimens and phylogenetic relationships

3.1.1. Sampled specimens

The 71 species included in this study were represented by 4,319 individuals classified in five butterfly families (Hesperiidae, Nymphalidae, Papilioneidae, Pieridae, and Riodinidae) and one day-flying moth species for comparisons (Uraniidae). For all species, we measured their wing morphometrics and thermal buffering ability, as well as we obtained COI sequences for each species from our own sampling in Peru or from public databases. Specifically, there were 964 individuals (17 species) of Hesperiidae, 2,842 individuals (43 species) of Nymphalidae, 348 individuals (6 species) of Papilionidae, 129 individuals (2 species) of Pieridae, 20 individuals (2 species) of Riodinidae, and 16 individuals (1 species) of Uraniidae (Appendix table 1. Morphological characteristics**.**). This reflected the relative abundances and encounter rate of such species during the field work in Peru.

3.1.2. Phylogenetic relationships

To compare the evolutionary relationships among the studied groups, we inferred a maximum likelihood phylogenetic tree using the COI sequences. The program ModelFinder found that the first and second coding positions should be merged, and the best-fit substitution model was *"TIM"*, while the third coding position had the *"TIM2"* model as best-fitting. For the statistical support of our inferred phylogenetic relationships, there were more than 52% of internal nodes with ultrafast bootstrap values higher than 95%, which was good given the low amount of data used to infer the phylogeny of the six Lepidoptera families.

3.2. The morphological traits of the butterflies

All the morphometrics were measured using the software ImageJ v1.54 (Schneider, Rasband, and Eliceiri 2012), with the exception of the total wing areas, which were measured using the MATLAB script "wingImageProcessor 1.1".

The results were based upon our 71 sampled species, and it may be different when comparing to larger and more diverse populations. Hesperiidae had the highest mean wing loading at 0.016 ± 0.004, while Uraniidae obtained the lowest wing loading at 0.001. The observation for Hesperiidae was largely explained by their robust and heavy thoraces. Nymphalidae stood out with the highest aspect ratio of 2.050 ± 0.429, reflecting their typical elongated and narrow wings. Riodinidae and Hesperiidae had lower aspect ratios (1.582 ± 0.196 and 1.914 ± 0.265, respectively) compared to other families, suggesting that their wings are rounder, which might be linked to increased flight abilities. Meanwhile, Riodinidae possessed the smallest wing area at 4.219 ± 3.495 cm^2. Papilionidae exhibited the highest mean thorax

volume at 0.190 ± 0.086 cm^3. In contrast, Riodinidae had the smallest mean thorax volumes at 0.018 ± 0.017 cm^3 (

Appendix figure 1). A summary of the morphometric parameters per family is presented in Table 2.

Family	species per family	Number of individuals
Hesperiidae	17	959
Nymphalidae	43	2,831
Papilionidae	6	347
Pieridae	2	129
Riodinidae	2	20
Uraniidae	1	16

Table 1. Summary of total number of species per family and individuals among the species.

Family	Wing loading (TV/TA)	Aspect ratio (WL/WW)	Wing length (WL) (cm)	Wing width (WW) (cm)	Total area (TA) (cm^2)	Thorax volume (TV)(cm^3)
Hesperiidae (N = 17)	0.016 ± 0.004	1.914 ± 0.265	2.340 ± 0.331	1.230 ± 0.144	8.013 ± 1.466	0.128 ± 0.046
Nymphalidae (N = 43)	0.004 ± 0.002	2.050 ± 0.429	3.831 ± 1.292	1.959 ± 0.853	21.428 ± 17.878	0.069 ± 0.043
Papilionidae (N = 6)	0.007 ± 0.002	1.969 ±0.099	5.115 ±1.304	2.594 ±0.615	28.406 ±12.009	0.190 ±0.086
Pieridae (N= 2)	0.003 ±3e-04	2.004 ±0.132	3.270 ±0.135	1.633 ±0.040	15.208 ±1.975	0.038 ±7e-04
Riodinidae (N= 2)	0.004 ±0.001	1.582 ±0.196	1.702 ±0.602	1.060 ±0.249	4.219 ±3.495	0.018 ±0.017

Uraniidae (N=1)	0.001	1.968	4.987	2.534	34.772	0.030

Table 2. Summary of average morphological characteristics in centimeters (cm) including standard deviation (± SD) for each butterfly and moth family. The N indicated how many different species were measured for the morphological parameters.

3.3. Thermal buffering ability

The body temperature, air temperature and thermal buffering ability of the studied butterflies are summarized in Table 3 and Table 4. A linear regression model was applied to fit the relationship between the air temperature and butterfly body temperature for each sampled species/subspecies.This analysis aimed to determine the slope of the fitted linear regression, which serves as an indicator of the buffering ability of butterflies (Bladon et al. 2020); the higher the thermal buffering ability results in a lower slope value of the fitted model. Overall, for our dataset, Pieridae had the highest average body temperature (T_b) at 32.29 ± 4.29 °C. Conversely, Nymphalidae exhibited the lowest T_b at 27.90 ± 3.25°C. In terms of air temperature (T_a), Pieridae also had the highest mean at 27.47 ± 2.67 °C. Meanwhile, Riodinidae showed the lowest average T_a at 24.74 ± 2.69 °C, in line with their propensity to occupy cooler micro-environments (e.g., resting under leaves of forest vegetation).

Family	average_Tbody	Min_Tbody	Max_Tbody	average_Tair	Min_Tair	Max_Tair	SD_Tbody	SD_Tair
Hesperiidae	31.95	20.00	43.00	26.05	18.00	33.30	3.80	2.56
Nymphalidae	27.90	16.60	39.30	25.11	15.30	35.20	3.25	2.51
Papilionidae	30.29	20.30	40.30	25.48	20.00	32.10	4.16	2.34
Pieridae	32.29	21.80	39.10	27.47	20.40	31.90	4.29	2.67
Riodinidae	29.80	22.80	37.50	24.74	18.30	29.20	4.63	2.69
Uraniidae	29.43	26.40	34.40	26.59	24.20	32.20	2.04	2.39

Table 3. Summary of average recorded temperatures in degree Celsius (°C). The table presents a summary of both body temperature (Tb) and air temperature (Ta) for six butterfly and moth families. It includes the maximum, minimum, average and standard deviation of temperature values.

	Mean slope	Min slope	Max slope
Hesperiidae	1.09	0.53	2.55
Nymphalidae	0.94	0.33	1.91

Papilionidae	1.03	0.88	1.24
Pieridae	0.97	0.88	1.05
Riodinidae	0.72	0.66	0.78
Uraniidae	0.77	0.77	0.77
Between_species	0.97	0.33	2.55

Table 4. Results of the linear regression models. Models describing dependence of the T_b on T_a (Appendix code 7 and Appendix code 8). The table summarizes the mean (average), minimum, and maximum values of slope parameters of each species per family and across all families (between species); the lower the slope of the fitted linear regression ($T_b \sim T_a$), the higher the thermal buffering ability.
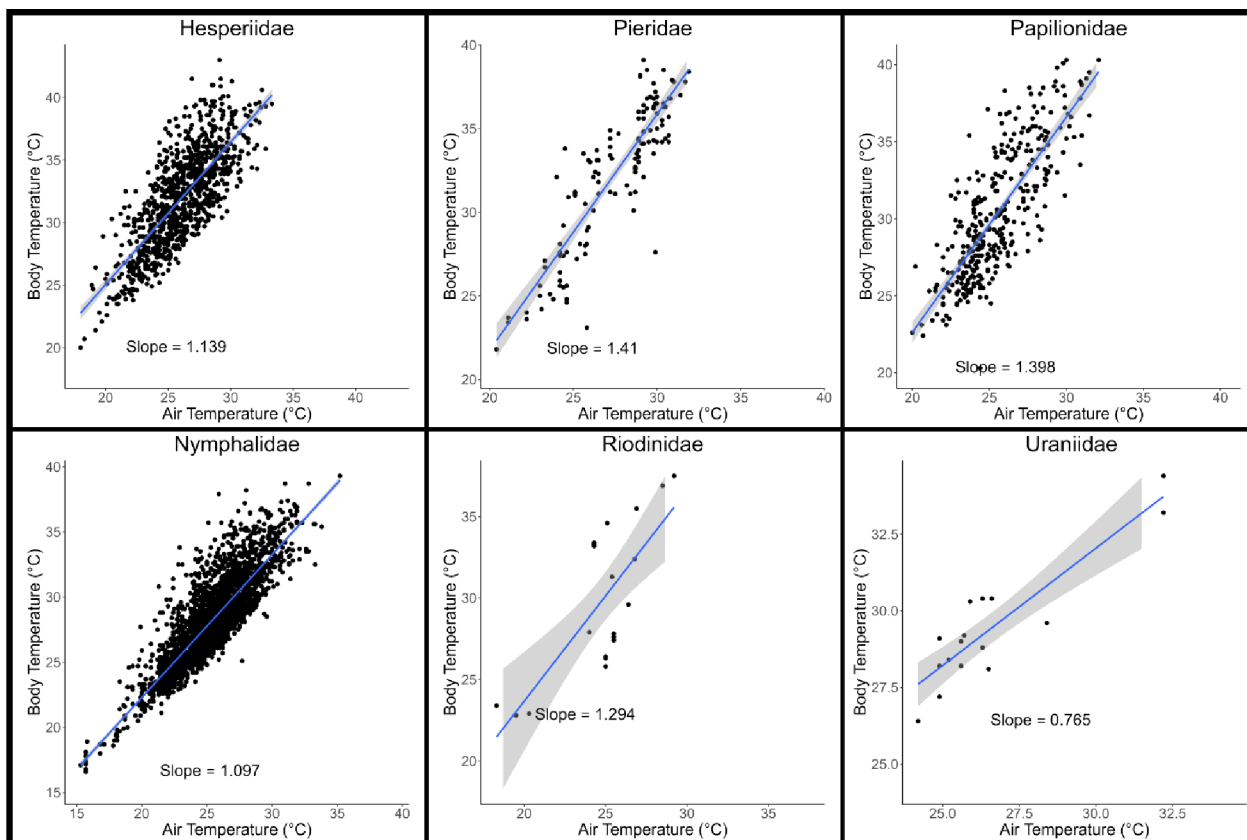

Figure 4. Butterfly body temperature (°C) variations at different ambient temperatures (°C) for each family (Appendix code 6). The solid blue lines display the fitted linear regression and the slope using function lm($T_b \sim T_a$) of such a relation is considered as a proxy for thermal buffering ability. The region surrounding the fitted regression line denotes the 95% confidence interval band.

The linear regression model applied to $T_b \sim T_a$ resulted in slopes that can be used as proxies to understand how body temperatures of each species per family change compared to the air temperature. On average, buffering abilities species across the families exhibited nearly 0.97± 0.32. Notably, species exhibited diverse thermal buffering abilities, ranging from regression slopes of around 0.33 (*Morpho menelaus*, Nymphalidae) to approximately 2.55 (*Elbella blue*, Hesperiidae). Among families, Hesperiidae recorded the highest per-species mean slope with 1.09 ± 0.49 ranging from 0.53 to 2.55, which implies their strong dependence to

ambient temperature (i.e., less buffering ability), however, their lifestyle should be considered as potentially relying more on behavioral thermoregulation as they might heat up rapidly thanks to their large thoracic muscles and their fast flight speed might allow them to cool down slowly. Contrarily, Riodinidae had the lowest per-species average slope at 0.72 ± 0.09 ranging from 0.66 to 0.78 (Table 4), implying a high buffering ability.
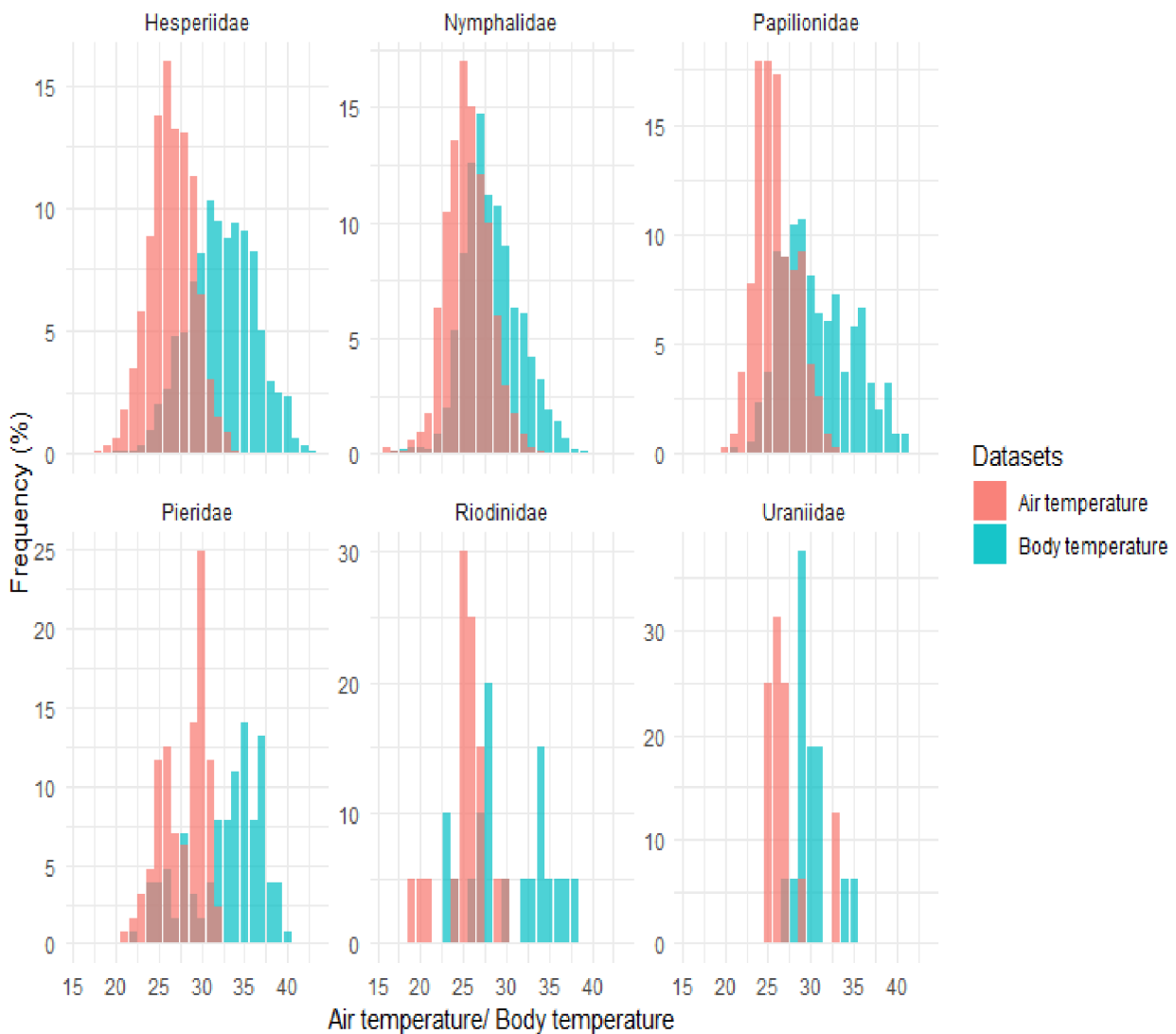
Figure 5. Bar plot depicting the distributions of body temperature and air temperature from a range of 10 °C to 40 °C by butterflies and moth family with the frequency of each T_a and T_b appearing within the family Appendix code 9 and Appendix code 10). It indicates that each family responded differently with the ambient temperature. Notably, Hesperiidae, Papilionidae, Pieridae, and Riodinidae exhibited significantly higher temperatures than the ambient air conditions that these species encountered. While Nymphalidae and Uraniidae were more stable compared to their air temperatures.

3.4. Does buffering ability correlate with butterfly morphology?

To assess the hypothesis on whether the butterfly morphometrics predict the thermal buffering ability of species, we used two phylogenetic comparative methods, Phylogenetic Independent Contrasts (PIC, Felsenstein 1985a) and Phylogenetic Generalized Least Squares (PGLS, Martins and Hansen 1997). Overall, the results produced by either method remained highly congruent.

Thermal Buffering vs.	P-value	Slope (without the intercept)
Wing loading	0.421	-0.051
Aspect ratio	**0.033**	**-0.304**
Total area	0.927	-0.008
Thoracic volume	0.458	-0.040

Table 5. Results of the linear regressions by species. Models describing dependence of the buffering ability (slope) on the morphometrics (wing loading, aspect ratio, etc.). The table shows the effect of morphological characteristics (wing loading, aspect ratio, total area, and thoracic volume) on the thermal buffering ability. The model was applied via the R function *gls*()and accounting for the effect of phylogeny via correlation of Brownian to fit the data (PGLS). In bold, the aspect ratio had a significant effect on per-species thermal buffering ability.

The aspect ratio of the species showed a significant effect (p-value ~0.033) on predicting the variation in butterfly buffering ability per species. The slope of the fitted regression was -0.304, which suggested that there is a significantly negative trend between the aspect ratio and the slope. All other morphological characteristics did not have a significant explanatory power for buffering ability. Furthermore, the approximate evolution of each trait along the phylogeny of the 71 sampled species/subspecies was visualized using the function *contMap()* from the R package *phytools*. The Felsenstein (1985) method was used to plot the reconstructed ancestral trait states for every internal node reconstructed and along branches in the maximum likelihood tree (Appendix figure 2 to Appendix figure 5).
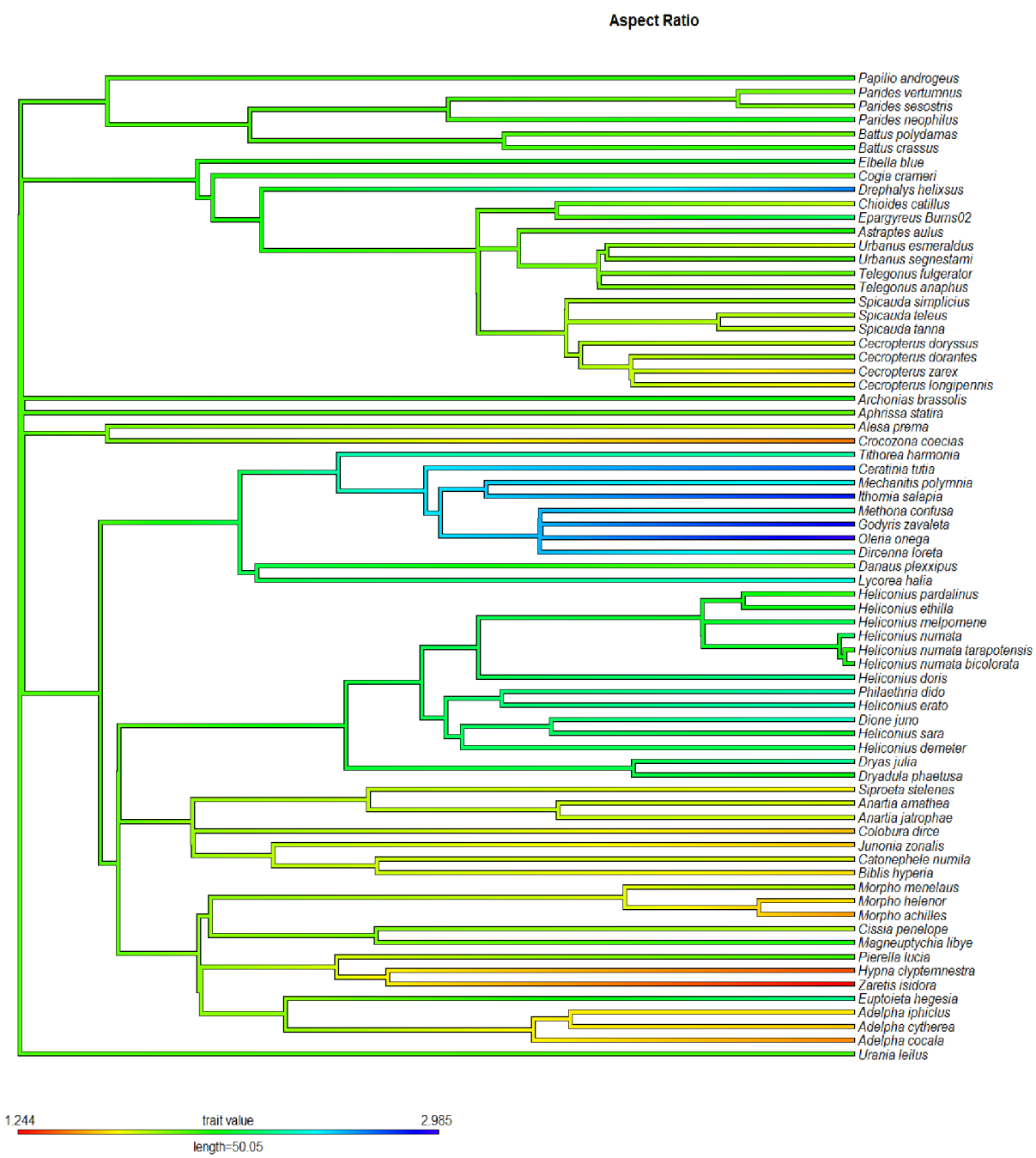
Aspect Ratio

Figure 6. Ancestral character state reconstruction for aspect ratio (forewing length divided by the forewing width). Colors represent low (red), intermediate (green), and high (blue) values of aspect ratio (the higher the aspect ratio the more elongated and narrower the forewings).

4. Discussion

Our aim was to determine whether wing morphometrics are good predictors for the estimated thermal buffering ability of tropical butterflies found in the Andean foothills. This suggests that butterflies w
ith greater aspect ratio (elongated and narrow forewings) correlates with increased thermal buffering ability (Table 5). Our finding might be explained by behavioral regulation of butterfly body temperatures, because species with high aspect ratio are often associated with gliding flight behavior (Le Roy, Debat, and Llaurens 2019). In our case, we found that while all butterfly families experienced similar ambient air temperatures, Hesperiidae tended to have higher T_b compared to others (right shifted Poisson distribution; Figure 5). Hesperiidae and other butterflies with rounded wings (i.e., low aspect ratio) may actively elevate their body temperatures by basking behavior and flight activity (Srygley and Chai 1990). The findings revealed the different thermoregulation abilities between the families, highlighting Nymphalidae as one with the largest aspect ratio among families. In the thesis, overall, we did not find evidence for ecomorphological traits, except for the forewing aspect ratio, being good predictors of thermal buffering ability.

This study is an important first step to estimate thermal buffering abilities of lower montane butterfly communities, which, thanks to our standardized and reproducible approach, can be compared to other studies (Laird-Hopkins et al., 2023; Ashe-Jepson et al., 2023). Nonetheless, the limitation of our approach was that we relied on photographic databases to measure the wing morphometrics of many of our studied butterflies. This limited the thesis to a subset of all recorded species (71 species), as it was challenging for us to collect all morphometrics of all the sampled species. Furthermore, the morphological traits examined in our study did not include the variability among individuals within species. Future studies should aim to collect such data by measuring the morphometrics on more reliable resources, such as freshly collected specimens, and to include the variation in morphological characteristics within species.

The diversity in thermoregulation abilities of species might be driven by their phylogeny (physiological constraint), morphology and behavior. Distinguishing the individual effects of these factors is not trivial, with each element playing a nuanced role. For example, *Erebia* butterflies in temperate regions present variations in thermoregulation abilities that were associated with differences in their habitat preferences (Kleckova and Klecka, 2016). This can be reconciled with other studies reporting similar patterns, and which may suggest that physical constraints such as body size play a more crucial role on the thermal requirements for flight (Nève and Hall 2016).

Our results indicated that the wing loading (predicting fast flight) and body size (wing area, thorax volume) had non-significant correlations with the thermal buffering ability of tropical butterflies (Table 5). Although we did not expect this outcome, as wing loading (fast flight) and large body size are usually correlated with low thermal buffering ability in other animals (Dyer et al. 2023), we cannot rule the alternative as our sampling size was low and focused on a single locality. In butterflies, however, buffering ability might be also due to behavioral rather than morphological features. Perhaps, active microhabitat choice plays a more

important role in determining the buffering ability in certain butterfly groups than the examined ecomorphological characteristics. Notably, butterflies with long elongated wings were found more frequently in the tropical climates than in the temperate regions (Laird-Hopkins et al. 2023). In future studies, it would be important to record the habitat preferences, temperature of microhabitats, and behavioral responses of butterflies to accurately predict how they would cope with the ongoing climate change. We, nonetheless, recovered strong evidence that butterflies with high buffering ability were strongly associated with greater wing aspect ratio. The results were also found in other tropical species where large winged butterflies had stronger thermal buffering abilities than small butterflies (Ashe-Jepson et al. 2023). Alternatively, most of the elongated and narrow wing butterflies such as Ithomiini and Heliconiini (Nymphalidae), are known to be unpalatable, which are often associated with slow movement (Srygley and Chai 1990). Both traits, nonetheless, could have evolved together as part of a multifaceted survival strategy, providing these butterflies with a dual advantage in terms of protection against predators and environmental challenges. However, to predict the likely responses of butterflies with high aspect ratio to climate change, further measures should be taken, including their thermal tolerance, which can be important for persisting during climatic extremes (Ashe-Jepson et al. 2023).

Under the scenario of climatic extremes, for example during heatwaves, butterflies typically hide in the shade, which hinders their ability to fly, feed or mate during such conditions, with potential long-term impacts (Hayes et al. 2023). For example, during hot weather events in the UK, butterflies were less active and more likely to hide than on subsequent 'normal' days (Hayes et al. 2023). Therefore, microclimate variability in the habitat, together with thermoregulation traits of butterflies, would be crucial for species to cope with future heatwave events and the ongoing climate change (Kleckova and Klecka 2016).

Studying the thermal buffering abilities and thermal tolerances of species occurring along environmental gradients is important to untangle the roles of behavioral variation and physiological constraints. For instance, *Heliconius* species from different elevations had different temperature tolerances (Montejo-Kovacevich et al. 2020). However, when these butterflies were raised in controlled environmental conditions, the differences decreased, suggesting that such species possess thermal plasticity leading to variation of thermal buffering ability along altitudes. The evidence suggests that butterflies living at high altitudes with low temperatures were better resistant to the cold than to heat, which might be an adaptive evolutionary response (Karl, Janowitz, and Fischer 2008). Crucially, heat stress resistance traits demonstrated notable flexibility, indicating a possible ability for adaptive changes in response to environmental conditions (Sørensen, Dahlgaard, and Loeschcke 2001). Therefore, when predicting the responses of species to temperature fluctuations, whether brief (extremely hot or cold periods) or prolonged (such as global warming), it is essential to account for both genetic adaptation and plasticity of the thermal abilities. This underscores the capacity of animals to adapt to temperature shifts through a combination of genetic modifications and short-term physiological and behavioral adaptations. In conclusion,

thermoregulation of ectotherms has complex and intertwined mechanisms, which can both reflect and influence the specific habitats and resource exploration preferences of different species or families (for example, Hesperiidae having high wing loading and body sizes, weakly correlated with buffering ability, while Ithomiini having elongated, and narrow wings are strongly correlated with improved buffering ability).

5. Conclusions

- The results showed that there were variations in thermal buffering ability between and among butterfly and moth families.

- Overall, after accounting for the effect of phylogeny, Nymphalidae had the larger aspect ratio compared to other families in our samples.

- Traditional morphological indicators of thermal resilience, such as fast flight and large body size, might not necessarily correlate with effective thermal buffering in butterflies. However, we found strong evidence that the aspect ratio of the forewings is positively correlated with the thermal buffering ability of the sampled species.

The thesis provided a standardized and reproducible approach for other studies that focus on measuring thermal buffering ability on lower montane butterfly communities. Future studies should focus on collecting these data in long term field works as well as in other environmental tropical gradients such as higher altitudes or a gradient of habitats, microhabitat choices (e.g., in butterfly sitting), record flight speed and escape abilities of butterflies. Altogether, such multi-evidence data may provide insights into the differences in thermoregulation mechanisms among butterfly species. The findings from this study offer insights of how butterflies handle temperature challenges by their adaptive strategies. As ongoing climate changes, the predictors of how butterflies respond to the environment become vital for conservation efforts and ecology.

6. Literature

Altschul, Stephen F., Warren Gish, Webb Miller, Eugene W. Myers, and David J. Lipman. 1990. "Basic Local Alignment Search Tool." *Journal of Molecular Biology* 215 (3): 403–10. https://doi.org/10.1016/S0022-2836(05)80360-2.

Ashe-Jepson, Esme, Stephany Arizala Cobo, Yves Basset, Andrew J. Bladon, Irena Kleckova, Benita C. Laird-Hopkins, Alex Mcfarlane, et al. 2023. "Tropical Butterflies Use Thermal Buffering and Thermal Tolerance as Alternative Strategies to Cope with Temperature Increase." *Journal of Animal Ecology* 92 (9): 1759–70. https://doi.org/10.1111/1365-2656.13970.

Barton, Madeleine, Warren Porter, and Michael Kearney. 2014. "Behavioural Thermoregulation and the Relative Roles of Convection and Radiation in a Basking Butterfly." *Journal of Thermal Biology* 41 (April): 65–71. https://doi.org/10.1016/j.jtherbio.2014.02.004.

Bladon, Andrew J., Matthew Lewis, Eleanor K. Bladon, Sam J. Buckton, Stuart Corbett, Steven R. Ewing, Matthew P. Hayes, et al. 2020. "How Butterflies Keep Their Cool: Physical and Ecological Traits Influence Thermoregulatory Ability and Population Trends." *Journal of Animal Ecology* 89 (11): 2440–50. https://doi.org/10.1111/1365-2656.13319.

Byrne, Michael P. 2021. "Amplified Warming of Extreme Temperatures over Tropical Land." *Nature Geoscience* 14 (11): 837–41. https://doi.org/10.1038/s41561-021-00828-8.

De Keyser, Rien, Casper J. Breuker, Rosemary S. Hails, Roger L. H. Dennis, and Tim G. Shreeve. 2015. "Why Small Is Beautiful: Wing Colour Is Free from Thermoregulatory Constraint in the Small Lycaenid Butterfly, Polyommatus Icarus." *PLoS ONE* 10 (4): e0122623. https://doi.org/10.1371/journal.pone.0122623.

Dongmo, Michel A. K., Rachid Hanna, Thomas B. Smith, K. K. M. Fiaboe, Abraham Fomena, and Timothy C. Bonebrake. 2021. "Local Adaptation in Thermal Tolerance for a Tropical Butterfly across Ecotone and Rainforest Habitats." *Biology Open* 10 (4): bio058619. https://doi.org/10.1242/bio.058619.

Dyer, Alexander, Ulrich Brose, Emilio Berti, Benjamin Rosenbaum, and Myriam R. Hirt. 2023. "The Travel Speeds of Large Animals Are Limited by Their Heat-Dissipation Capacities." *PLOS Biology* 21 (4): e3001820. https://doi.org/10.1371/journal.pbio.3001820.

Felsenstein, Joseph. 1985. "Phylogenies and the Comparative Method." *The American Naturalist* 125 (1): 1–15.

García-Barros, Enrique. 2015. "Multivariate Indices as Estimates of Dry Body Weight for Comparative Study of Body Size in Lepidoptera." *Nota Lepidopterologica* 38 (1): 59–74. https://doi.org/10.3897/nl.38.8957.

Grinder, Rollie M., and John J. Wiens. 2023. "Niche Width Predicts Extinction from Climate Change and Vulnerability of Tropical Species." *Global Change Biology* 29 (3): 618–30. https://doi.org/10.1111/gcb.16486.

Hayes, Matthew P., Esme Ashe-Jepson, Gwen E. Hitchcock, Ryan Clark, Josh Hellon, Richard I. Knock, Andrew J. Bladon, and Edgar C. Turner. 2023. "Heatwave Predicts a Shady Future for Insects: Impacts of an Extreme Weather Event on a Chalk Grassland in Bedfordshire, UK." Preprint. In Review. https://doi.org/10.21203/rs.3.rs-3462943/v1.

Hoang, Diep Thi, Olga Chernomor, Arndt von Haeseler, Bui Quang Minh, and Le Sy Vinh. 2018. "UFBoot2: Improving the Ultrafast Bootstrap Approximation." *Molecular Biology and Evolution* 35 (2): 518–22. https://doi.org/10.1093/molbev/msx281.

Johansson, Frank, Germán Orizaola, and Viktor Nilsson-Örtman. 2020. "Temperate Insects with Narrow Seasonal Activity Periods Can Be as Vulnerable to Climate Change as Tropical Insect Species." *Scientific Reports* 10 (1): 8822. https://doi.org/10.1038/s41598-020-65608-7.

Karl, Isabell, Susann A. Janowitz, and Klaus Fischer. 2008. "Altitudinal Life-History Variation and Thermal Adaptation in the Copper Butterfly Lycaena Tityrus." *Oikos* 117 (5): 778–88. https://doi.org/10.1111/j.0030-1299.2008.16522.x.

Katoh, Kazutaka, and Daron M. Standley. 2013. "MAFFT Multiple Sequence Alignment Software Version 7: Improvements in Performance and Usability." *Molecular Biology and Evolution* 30 (4): 772–80. https://doi.org/10.1093/molbev/mst010.

Kawahara, Akito Y., Caroline Storer, Ana Paula S. Carvalho, David M. Plotkin, Fabien L. Condamine, Mariana P. Braga, Emily A. Ellis, et al. 2023. "A Global Phylogeny of Butterflies Reveals Their Evolutionary History, Ancestral Hosts and Biogeographic Origins." *Nature Ecology & Evolution* 7 (6): 903–13. https://doi.org/10.1038/s41559-023-02041-9.

Kellermann, Vanessa, and Belinda van Heerwaarden. 2019. "Terrestrial Insects and Climate Change: Adaptive Responses in Key Traits." *Physiological Entomology* 44 (2): 99–115. https://doi.org/10.1111/phen.12282.

Kleckova, Irena, and Jan Klecka. 2016. "Facing the Heat: Thermoregulation and Behaviour of Lowland Species of a Cold-Dwelling Butterfly Genus, Erebia." *PLOS ONE* 11 (3): e0150393. https://doi.org/10.1371/journal.pone.0150393.

Laird-Hopkins, Benita, Esme Ashe-Jepson, Yves Basset, Stephany Arizala Cobo, Lucy Eberhardt, Inga Freiberga, Josh Hellon, et al. 2023. "Thermoregulatory Ability and Mechanism Do Not Differ Consistently between Neotropical and Temperate Butterflies." *Global Change Biology* 29 (June). https://doi.org/10.1111/gcb.16797.

Le Roy, Camille, Vincent Debat, and Violaine Llaurens. 2019. "Adaptive Evolution of Butterfly Wing Shape: From Morphology to Behaviour." *Biological Reviews* 94 (4): 1261–81. https://doi.org/10.1111/brv.12500.

Martins, Emilia P., and Thomas F. Hansen. 1997. "Phylogenies and the Comparative Method: A General Approach to Incorporating Phylogenetic Information into the Analysis of Interspecific Data." *The American Naturalist* 149 (4): 646–67. https://doi.org/10.1086/286013.

Matos-Maraví, Pável F., Carlos Peña, Keith R. Willmott, André V. L. Freitas, and Niklas Wahlberg. 2013. "Systematics and Evolutionary History of Butterflies in the 'Taygetis Clade' (Nymphalidae: Satyrinae: Euptychiina): Towards a Better Understanding of Neotropical Biogeography." *Molecular Phylogenetics and Evolution* 66 (1): 54–68. https://doi.org/10.1016/j.ympev.2012.09.005.

Minh, Bui Quang, Heiko A Schmidt, Olga Chernomor, Dominik Schrempf, Michael D Woodhams, Arndt von Haeseler, and Robert Lanfear. 2020. "IQ-TREE 2: New Models and Efficient Methods for Phylogenetic Inference in the Genomic Era." *Molecular Biology and Evolution* 37 (5): 1530–34. https://doi.org/10.1093/molbev/msaa015.

Montejo-Kovacevich, Gabriela, Simon H. Martin, Joana I. Meier, Caroline N. Bacquet, Monica Monllor, Chris D. Jiggins, and Nicola J. Nadeau. 2020. "Microclimate Buffering and Thermal Tolerance across Elevations in a Tropical Butterfly." *Journal of Experimental Biology* 223 (8): jeb220426. https://doi.org/10.1242/jeb.220426.

Nève, Gabriel, and Casey Hall. 2016. "Variation of Thorax Flight Temperature among Twenty Australian Butterflies (Lepidoptera: Papilionidae, Nymphalidae, Pieridae, Hesperiidae, Lycaenidae)." *EJE* 113 (1): 571–78. https://doi.org/10.14411/eje.2016.077.

Nugent, Cam. (2019) 2019. "BOLD-CLI." Go. https://github.com/CNuge/BOLD-CLI.

Orme [aut, David, cre, Rob Freckleton, Gavin Thomas, Thomas Petzoldt, Susanne Fritz, Nick Isaac, and Will Pearse. 2023. "Caper: Comparative Analyses of Phylogenetics and Evolution in R." https://cran.r-project.org/web/packages/caper/index.html.

Paradis, Emmanuel, and Klaus Schliep. 2019. "Ape 5.0: An Environment for Modern Phylogenetics and Evolutionary Analyses in R." *Bioinformatics* 35 (3): 526–28. https://doi.org/10.1093/bioinformatics/bty633.

Pinheiro, José C., and Douglas M. Bates, eds. 2000. "Fitting Nonlinear Mixed-Effects Models." In *Mixed-Effects Models in S and S-PLUS*, 337–421. Statistics and Computing. New York, NY: Springer. https://doi.org/10.1007/0-387-22747-4_8.

R Core Team 2023. n.d. "R: The R Project for Statistical Computing." https://www.r-project.org/.

Revell, Liam J. 2012. "Phytools: An R Package for Phylogenetic Comparative Biology (and Other Things)." *Methods in Ecology and Evolution* 3 (2): 217–23. https://doi.org/10.1111/j.2041-210X.2011.00169.x.

Rodrigues, Meghie. 2023. "The Amazon's Record-Setting Drought: How Bad Will It Be?" *Nature*, November. https://doi.org/10.1038/d41586-023-03469-6.

Schneider, Caroline A., Wayne S. Rasband, and Kevin W. Eliceiri. 2012. "NIH Image to ImageJ: 25 Years of Image Analysis." *Nature Methods* 9 (7): 671–75. https://doi.org/10.1038/nmeth.2089.

Sørensen, J. G., J. Dahlgaard, and V. Loeschcke. 2001. "Genetic Variation in Thermal Tolerance among Natural Populations of Drosophila Buzzatii: Down Regulation of Hsp70 Expression and Variation in Heat Stress Resistance Traits." *Functional Ecology* 15 (3): 289–96. https://doi.org/10.1046/j.1365-2435.2001.00525.x.

Srygley, Robert B., and Peng Chai. 1990. "Predation and the Elevation of Thoracic Temperature in Brightly Colored Neotropical Butterflies." *The American Naturalist* 135 (6): 766–87.

Wickham, Hadley, Romain François, Lionel Henry, Kirill Müller, Davis Vaughan, Posit Software, and PBC. 2023. "Dplyr: A Grammar of Data Manipulation." https://cran.r-project.org/web/packages/dplyr/index.html.

Xing, Shuang, Timothy C. Bonebrake, Chin Cheung Tang, Evan J. Pickett, Wenda Cheng, Sasha E. Greenspan, Stephen E. Williams, and Brett R. Scheffers. 2016. "Cool Habitats Support Darker and Bigger Butterflies in Australian Tropical Forests." *Ecology and Evolution* 6 (22): 8062–74. https://doi.org/10.1002/ece3.2464.
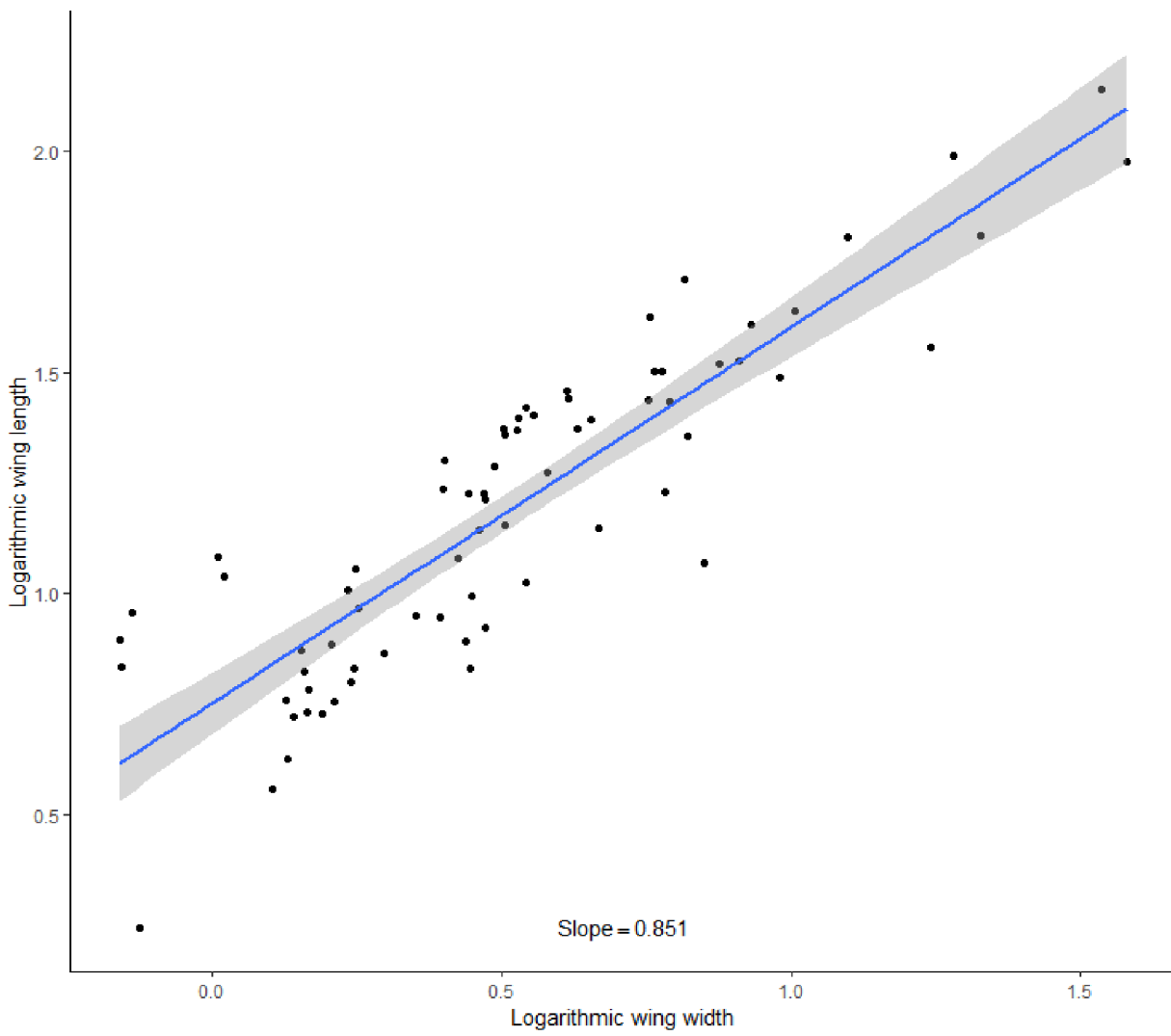
7. Figures

8. Tables

9. Appendix

Appendix table 1. Morphological characteristics.

	Family	species	wing_length (cm)	wing_width (cm)	aspect_ratio	front_wing_area (cm2)	hind_wing_area(cm2)	total_area(cm2)	thorax_length (cm)	throax_width (cm)	abdomen_width (cm)	abdomen_length (cm)	Thorax Cylinder volume	wing_loading
0	Rhiodiniidae	Crocozona coecias	1.2760	0.8840	0.693	0.8073	0.0664	1.7474	0.3760	0.1360	0.1140	0.5610	0.005462	0.003126
1	Nymphalidae	Oleria onega	2.6002	0.8711	0.335	2.0507	1.8848	7.8710	0.4007	0.1881	0.1312	1.1299	0.011135	0.001415
2	Hesperiidae	Cecropterus zarex	1.7500	1.1105	0.635	1.2367	1.2415	4.9604	0.9913	0.3352	0.2286	0.6749	0.087479	0.017635
3	Hesperiidae	Cecropterus longipennis	1.8710	1.1393	0.609	1.4162	1.4627	5.7578	0.6552	0.4109	0.1957	0.6773	0.086883	0.015090
4	Nymphalidae	Cissia penelope	2.0589	1.1533	0.560	1.5859	1.8536	6.8790	0.5017	0.1512	0.1795	0.6788	0.009008	0.001310
5	Hesperiidae	Urbanus esmeraldus	2.0747	1.2108	0.584	1.6853	2.3396	8.0498	0.8716	0.4276	0.2576	0.7531	0.125165	0.015649
6	Hesperiidae	Cecropterus doryssus	2.0774	1.1793	0.568	1.8165	1.6519	6.9368	0.7516	0.4429	0.1921	0.5459	0.115825	0.016697
7	Nymphalidae	Dryas julia	4.2967	1.8484	0.430	5.5576	3.6673	18.4498	0.6993	0.3365	0.0919	1.2011	0.061821	0.003351
8	Rhiodiniidae	Alesa prema	2.1279	1.2362	0.581	1.8727	1.4721	6.6896	0.6181	0.2483	0.1582	0.8748	0.029930	0.004474
9	Hesperiidae	Cecropterus dorantes	2.1354	1.1363	0.532	1.7860	1.9460	7.4640	0.8030	0.4530	0.1905	0.7385	0.129420	0.017339
10	Hesperiidae	Spicauda simplicius	2.1892	1.1821	0.540	1.7390	2.0292	7.5364	0.7819	0.3662	0.2201	0.7682	0.082353	0.010927
11	Hesperiidae	Spicauda tanna	2.2304	1.2724	0.570	1.7106	1.8487	7.1186	0.7500	0.4655	0.1640	0.6159	0.127641	0.017931
12	Hesperiidae	Cogia crameri	2.2608	1.1729	0.514	1.8589	2.0763	7.8704	0.7221	0.4120	0.3239	0.7449	0.096268	0.012232
13	Hesperiidae	Spicauda teleus	2.2936	1.2797	0.558	1.9622	2.0289	7.9822	0.8759	0.4341	0.2408	0.7135	0.129636	0.016241
14	Nymphalidae	Adelpha cocala	2.2955	1.5643	0.681	2.3732	2.7191	10.1845	0.6643	0.2475	0.1050	0.8481	0.031960	0.003138
15	Hesperiidae	Drephalys helixus	2.3070	0.8558	0.371	1.8180	1.8520	7.3410	0.8232	0.4459	0.3595	0.8365	0.128549	0.017512
16	Hesperiidae	Chioides catillus	2.3723	1.3467	0.568	1.9709	2.1784	8.2986	0.6956	0.4345	0.2915	0.7287	0.103140	0.012429
17	Nymphalidae	Magneuptychia libye	2.3892	1.1660	0.488	2.6539	2.8243	10.9564	0.5900	0.2492	0.1901	0.6388	0.026776	0.002626
18	Hesperiidae	Urbanus segnestami	2.4273	1.2306	0.507	2.2392	2.6873	9.8530	0.7603	0.2836	0.3869	0.9889	0.048027	0.004874
19	Nymphalidae	Adelpha cytherea	2.4401	1.5521	0.636	2.6375	2.4159	10.1068	0.5503	0.2367	0.1807	0.7348	0.024215	0.002396
20	Nymphalidae	Ithomia salapia	2.4494	0.8541	0.349	2.1204	1.1867	6.6182	0.4358	0.2363	0.1370	1.1791	0.019112	0.002688
21	Nymphalidae	Junonia zonalis	2.5177	1.6040	0.637	2.5441	2.6550	10.3982	0.6761	0.3348	0.2133	0.9699	0.059521	0.005724
22	Nymphalidae	Anartia jatrophae	2.5810	1.4820	0.574	2.5662	2.4541	10.0406	0.6260	0.2070	0.1500	0.7710	0.021067	0.002098
23	Hesperiidae	Telegonus anaphus	2.5907	1.4224	0.549	2.3077	2.0756	8.7666	0.8758	0.5537	0.3727	0.9386	0.210884	0.024055
24	Hesperiidae	Astraptes aulus	2.6312	1.2878	0.489	2.3187	2.2749	9.1872	0.9519	0.5208	0.2840	0.9517	0.202779	0.022072
25	Nymphalidae	Anartia amathea	2.7054	1.5649	0.578	2.6494	2.6443	10.5874	0.6295	0.3242	0.1529	0.6859	0.051965	0.004908
26	Hesperiidae	Elbella blue	2.7392	1.2670	0.463	2.4015	2.0086	8.8202	1.0331	0.4557	0.5390	1.1908	0.168496	0.019103
27	Nymphalidae	Adelpha iphiclus	2.7900	1.7186	0.616	3.1193	2.8875	12.0136	0.7658	0.2908	0.1822	0.9637	0.050862	0.004234
28	Nymphalidae	Ceratinia tutia	2.8230	1.0210	0.362	2.5500	1.4600	8.0200	0.5190	0.1970	0.1360	1.2870	0.015819	0.001972
29	Hesperiidae	Epargyreus Burns02	2.8722	1.2822	0.446	2.7110	1.8745	9.1710	0.7659	0.4649	0.4374	1.0153	0.130011	0.014176
30	Nymphalidae	Zaretis isidora	2.9139	2.3423	0.804	4.6245	4.0772	17.4034	0.8642	0.3310	0.2110	0.8760	0.074364	0.004273
31	Hesperiidae	Telegonus fulgerator	2.9392	1.5285	0.520	2.9916	2.5647	11.1126	0.8893	0.5386	0.4608	1.2203	0.202615	0.018233
32	Nymphalidae	Godyris zavaleta	2.9560	1.0120	0.342	2.8651	2.3236	10.3774	0.7250	0.2030	0.0970	1.4440	0.023465	0.002261
33	Nymphalidae	Pierella lucia	3.1429	1.5883	0.505	3.6667	4.0945	15.5224	0.4796	0.3728	0.0675	0.9951	0.052340	0.003372
34	Nymphalidae	Biblis hyperia	3.1536	1.9491	0.618	4.2497	3.9535	16.4064	0.6147	0.2401	0.1479	0.7898	0.027832	0.001696
35	Pieridae	Aphrissa statira	3.1742	1.6612	0.523	4.4053	3.8967	16.6040	0.6636	0.2719	0.1754	1.2528	0.038531	0.002321
36	Pieridae	Archonias brassolis	3.3649	1.6045	0.477	4.0853	2.8203	13.8112	0.7132	0.2590	0.0948	0.8627	0.037575	0.002721
37	Nymphalidae	Heliconius demeter	3.4049	1.5574	0.457	3.8025	2.3123	12.2296	0.7890	0.4801	0.1900	1.1900	0.142834	0.011679
38	Nymphalidae	Heliconius sara	3.4121	1.6005	0.469	3.9523	2.6856	13.2758	0.7160	0.3846	0.1231	1.3517	0.083413	0.006283
39	Nymphalidae	Coloburla dirce	3.4255	2.1854	0.638	6.0422	4.8001	21.6846	0.6318	0.3617	0.1701	1.2000	0.085468	0.003941
40	Nymphalidae	Euptoieta hegesia	3.4450	1.4920	0.433	4.7394	4.2654	18.0096	1.0480	0.1650	0.2890	0.7134	0.022409	0.001244
41	Nymphalidae	Heliconius pardalinus	3.5689	1.7868	0.501	4.5269	3.2059	15.4656	0.7359	0.3454	0.1619	1.3990	0.068953	0.004458
42	Nymphalidae	Heliconius melpomene	3.6178	1.6309	0.451	4.6828	3.2044	15.7744	0.6496	0.2968	0.1202	1.0986	0.044943	0.002849
43	Nymphalidae	Mechanitis polymnia	3.6716	1.4931	0.407	4.2368	2.5775	13.8286	0.5885	0.2670	0.0920	1.7893	0.032950	0.002383
44	Nymphalidae	Catonephele numila	3.8856	2.2727	0.585	5.1877	4.7139	19.8032	0.8929	0.3675	0.0780	1.2202	0.094713	0.004783
45	Nymphalidae	Methona confusa	3.8933	1.6600	0.426	4.3639	2.7262	14.1842	0.7941	0.3922	0.2969	1.5603	0.095936	0.006764
46	Nymphalidae	Heliconius doris	3.9376	1.6938	0.430	4.9484	3.3483	16.5934	0.8886	0.3805	0.1897	1.2045	0.101043	0.006089
47	Nymphalidae	Dircenna loreta	3.9469	1.6556	0.419	4.3212	2.2355	13.1134	0.7019	0.3392	0.0740	1.6628	0.063427	0.004837
48	Papilionidae	Parides neophilus	3.9502	1.8777	0.475	4.6530	2.4099	14.1258	0.8780	0.4396	0.3080	1.6860	0.133260	0.009434
49	Nymphalidae	Heliconius ethilla	4.0257	1.9229	0.478	5.5787	3.4108	17.9790	0.8153	0.3313	0.2143	1.6592	0.070283	0.003909
50	Nymphalidae	Heliconius erato	4.0347	1.6985	0.421	5.5375	3.9600	18.9950	0.7207	0.3675	0.0588	1.4320	0.076447	0.004025
51	Nymphalidae	Tithorea harmonia	4.0747	1.7452	0.428	6.7340	4.2107	21.8894	0.8547	0.3183	0.1736	1.3917	0.068011	0.003107
52	Nymphalidae	Dione juno	4.1383	1.7224	0.416	4.7863	4.2689	18.1104	0.6207	0.3126	0.3354	1.0604	0.047636	0.002630
53	Papilionidae	Parides vertumnus	4.1904	2.2026	0.526	6.4299	3.5961	20.0520	0.9784	0.3974	0.1975	1.4049	0.121356	0.006052
54	Nymphalidae	Heliconius numata tarapotensis	4.2060	2.1269	0.506	6.8791	4.2105	22.1792	0.7267	0.4463	0.2284	1.5535	0.113684	0.005126
55	Nymphalidae	Heliconius numata	4.2195	1.8517	0.439	6.6521	4.0954	21.4950	0.7739	0.3093	0.2930	1.7497	0.058148	0.002705
56	Nymphalidae	Siproeta stelenes	4.4325	2.6647	0.601	7.1120	5.9343	26.0926	0.6271	0.3847	0.1538	1.0214	0.096137	0.003684
57	Nymphalidae	Dryadula phaetusa	4.4880	2.1470	0.478	6.4265	5.9253	24.7036	0.9700	0.4670	0.1590	1.6210	0.166148	0.006726
58	Nymphalidae	Heliconius numata bicolorata	4.4924	2.1757	0.484	6.8945	4.6042	22.9974	0.8334	0.4585	0.2088	2.0067	0.137601	0.005983
59	Papilionidae	Battus polydamas	4.5661	2.4001	0.526	7.2221	6.2918	27.0278	1.0120	0.5666	0.3111	1.7005	0.255166	0.009441
60	Papilionidae	Parides sesostris	4.5929	2.4850	0.541	7.3229	4.6618	23.9694	0.9519	0.3788	0.3875	1.6222	0.107276	0.004476
61	Nymphalidae	Hypna clytemnestra	4.7375	3.4556	0.729	10.8315	10.4703	42.6036	0.8124	0.3698	0.3682	1.0433	0.087256	0.002048
62	Z-Uraniidae	Urania leilus	4.9870	2.5340	0.508	8.6191	8.7671	34.7724	0.6906	0.2334	0.3112	1.3831	0.029547	0.000850
63	Nymphalidae	Philaethria dido	5.0713	2.1297	0.420	6.9966	5.9212	25.2356	0.8873	0.4964	0.1945	1.1665	0.171721	0.006805
64	Nymphalidae	Danaus plexxipus	5.1430	2.7383	0.532	7.8825	7.8032	31.3714	1.1836	0.1953	0.1139	1.7586	0.035457	0.001130
65	Nymphalidae	Lycorea halia	5.5334	2.2631	0.409	9.5090	7.5410	34.1000	0.8715	0.3857	0.3084	2.3145	0.101825	0.002986
66	Papilionidae	Battus crassus	6.0906	3.0008	0.493	12.7784	6.9155	39.3878	1.3850	0.5464	0.5548	1.6630	0.324759	0.008245
67	Nymphalidae	Morpho helenor	6.1030	3.7740	0.618	16.7649	16.2059	65.9416	0.6771	0.4155	0.3892	1.2222	0.091809	0.001392
68	Nymphalidae	Morpho achilles	7.2126	4.8509	0.673	20.2970	19.7834	80.1608	0.7749	0.4078	0.4063	1.2277	0.101212	0.001263
69	Papilionidae	Papilio androgeus	7.2972	3.5975	0.493	13.7614	9.1765	45.8758	1.1766	0.4599	0.2819	1.8527	0.195454	0.004261
70	Nymphalidae	Morpho menelaus	8.4817	4.6447	0.548	27.5950	18.2877	91.7654	0.6651	0.5504	0.3797	1.4861	0.158246	0.001724

Appendix figure 1. The regression (blue line) depicting the positive relationship between the forewing width and length using *lm*() function. The region surrounding the fitted linear regression denotes the 95% confidence interval band.

Appendix figure 2. Ancestral character state reconstruction for total wing area (cm2). Colors represent low (red), intermediate (green), and high (blue) values of the total area (log).

Total Area (log)
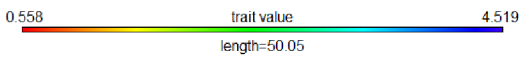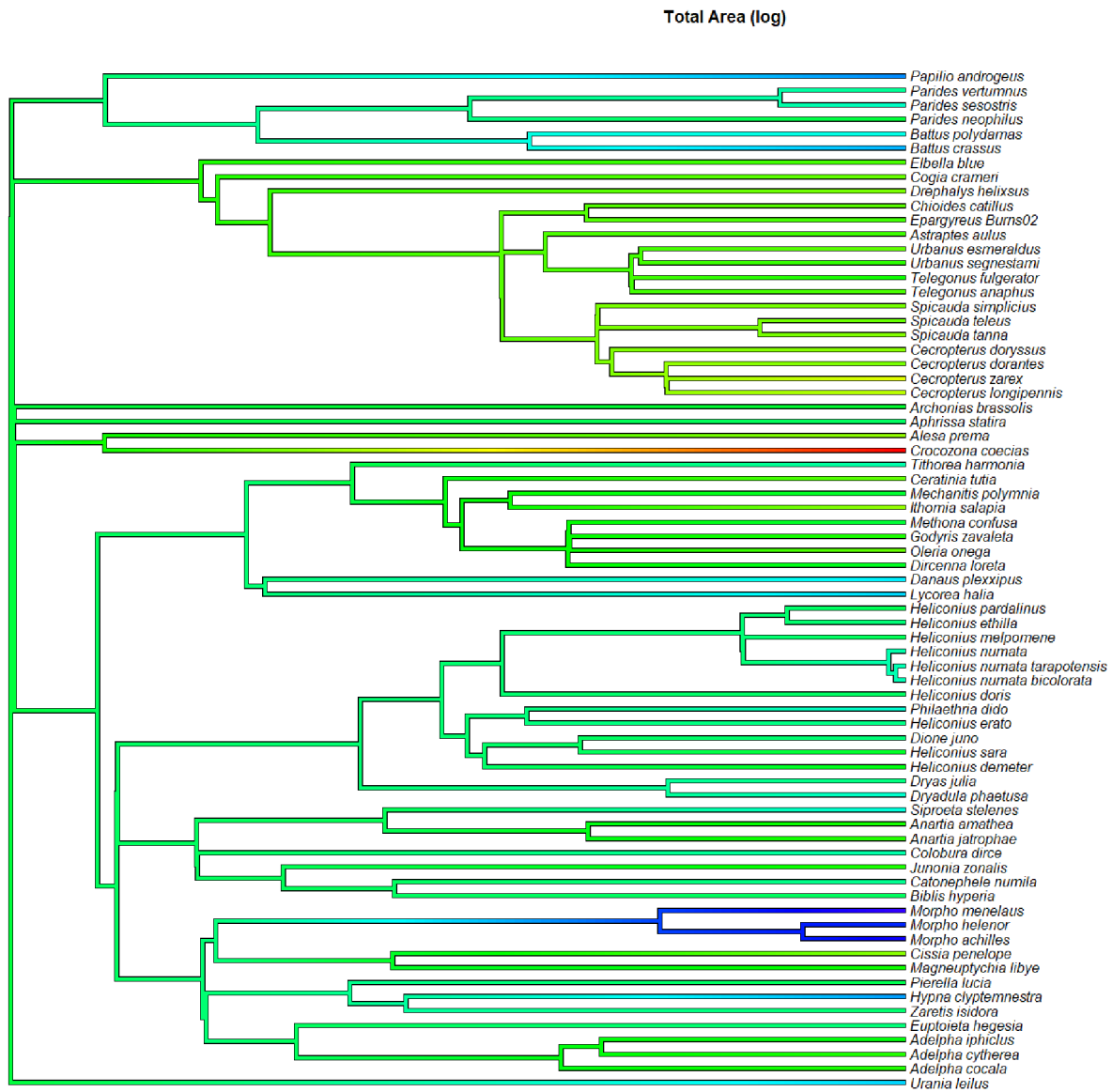
Appendix figure 3. Ancestral character state reconstruction for wing loading (thorax volume divided by the total wing area). Colors represent low (red), intermediate (green), and high (blue) values of wing loading (log).

Wing Loading (log)
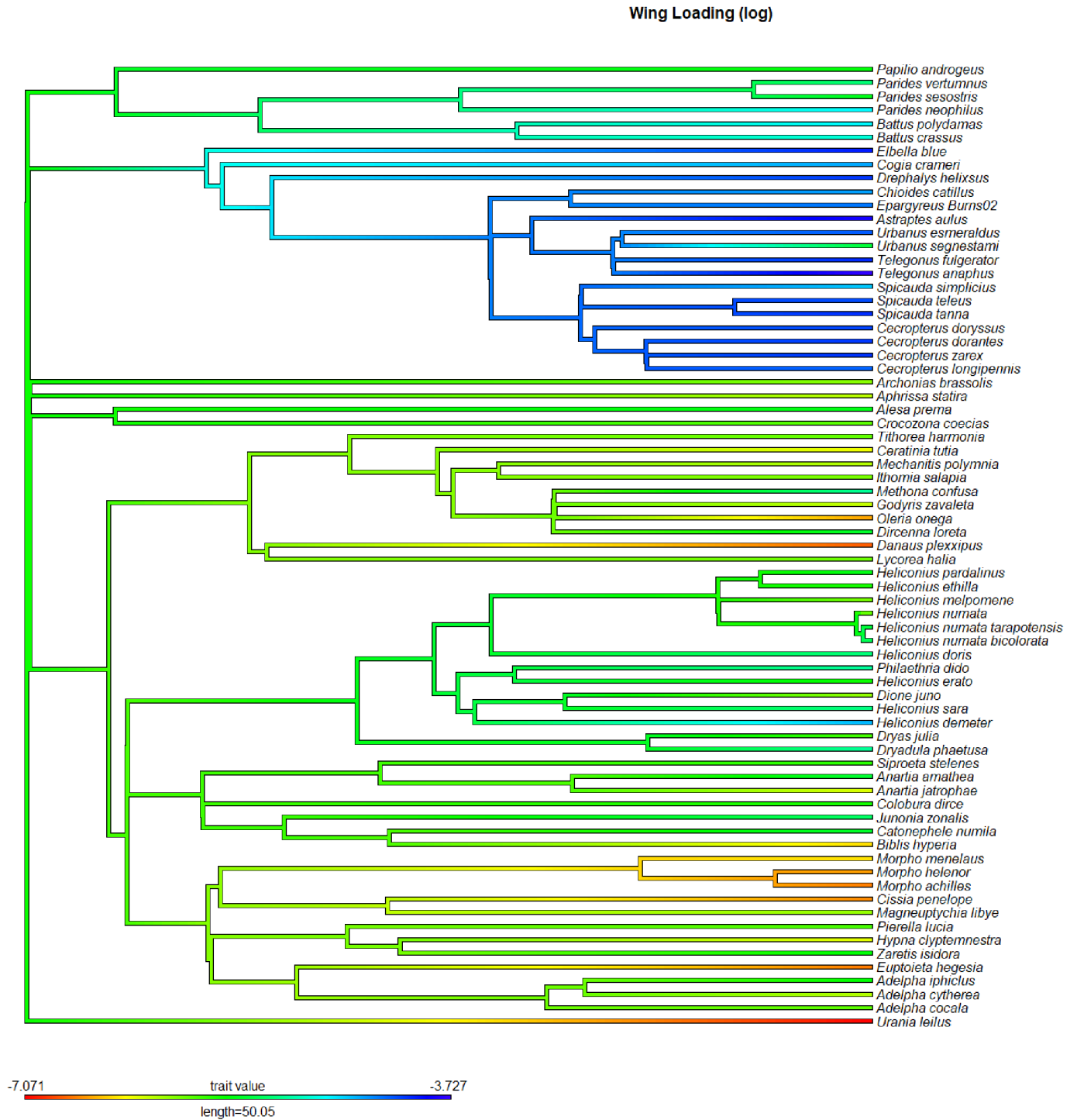
Appendix figure 4. Ancestral character state reconstruction for buffering ability (inversed slopes). Colors represent high (red), intermediate (green), and low (blue) estimated thermal buffering ability.

Buffering ability (Slopes)
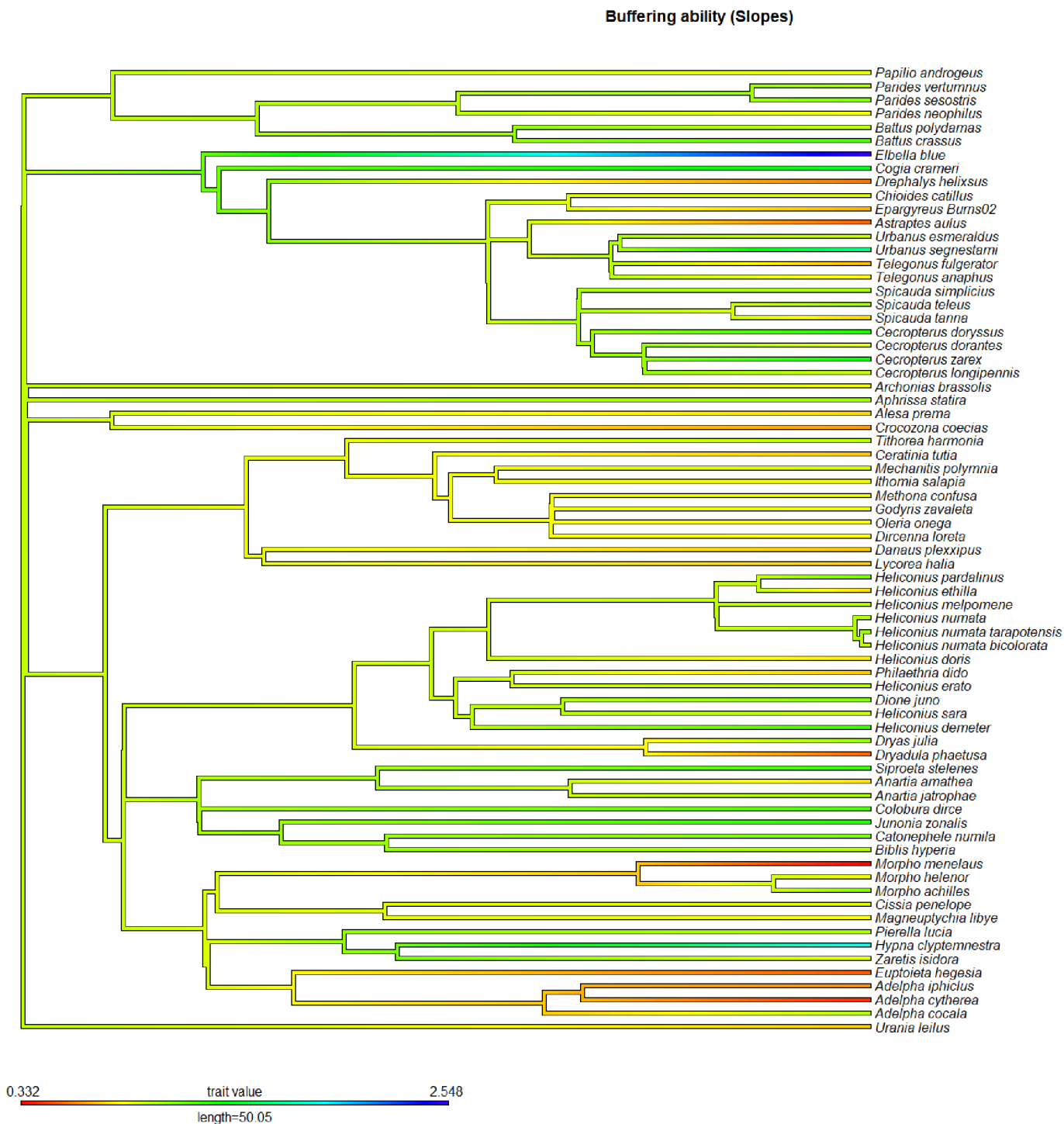
Appendix figure 5. Ancestral character state reconstruction for thorax volume (cm3). Colors represent low (red), intermediate (green), and high (blue) values of thorax cylinder volume (log).

Thorax Volume (log)

Papilio androgeus
Parides vertumnus
Parides sesostris
Parides neophilus
Battus polydamas
Battus crassus
Elbella blue
Cogia crameri
Drephalys helixsus
Choides catillus
Epargyreus Burns02
Astraptes aulus
Urbanus esmeraldus
Urbanus segnestami
Telegonus fulgerator
Telegonus anaphus
Spicauda simplicius
Spicauda teleus
Spicauda tanna
Cecropterus doryssus
Cecropterus dorantes
Cecropterus zarex
Cecropterus longipennis
Archonias brassolis
Aphrissa statira
Alesa prema
Crocozona coecias
Tithorea harmonia
Ceratinia tutia
Mechanitis polymnia
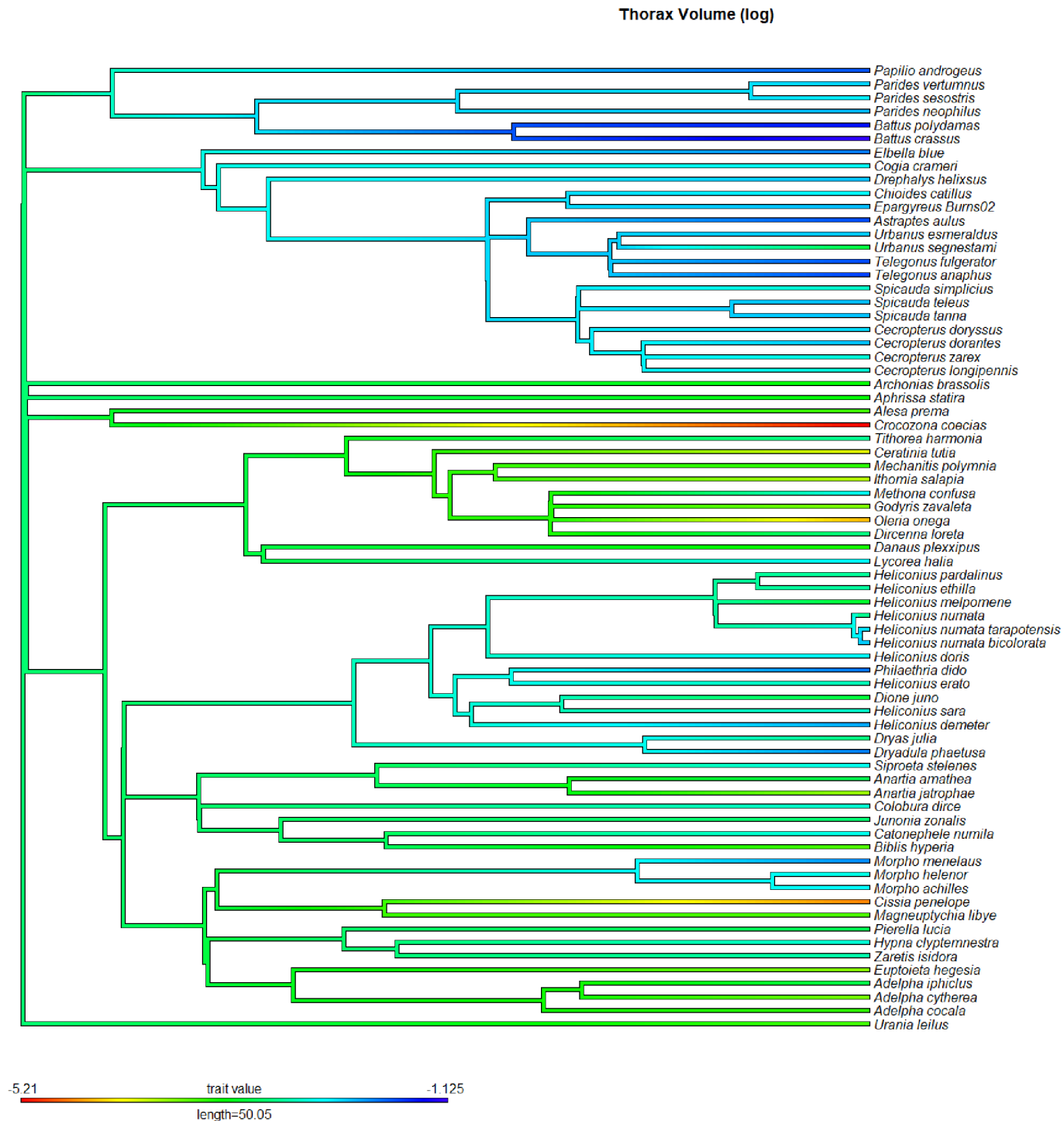*Ithomia salapia*
Methona confusa
Godyris zavaleta
Oleria onega
Dircenna loreta
Danaus plexxipus
Lycorea halia
Heliconius pardalinus
Heliconius ethilla
Heliconius melpomene
Heliconius numata
Heliconius numata tarapotensis
Heliconius numata bicolorata
Heliconius doris
Philaethria dido
Heliconius erato
Dione juno
Heliconius sara
Heliconius demeter
Dryas julia
Dryadula phaetusa
Siproeta stelenes
Anartia amathea
Anartia jatrophae
Colobura dirce
Junonia zonalis
Catonephele numila
Biblis hyperia
Morpho menelaus
Morpho helenor
Morpho achilles
Cissia penelope
Magneuptychia libye
Pierella lucia
Hypna clypternnestra
Zaretis isidora
Euptoieta hegesia
Adelpha iphiclus
Adelpha cytherea
Adelpha cocala
Urania leilus

-5.21   trait value   -1.125

length=50.05

Appendix code 1.BOLD-CLI command to retrive the databases on BOLD Systems for butterflies.

```
bold-cli -query sequence -output ./Datasets/Seq2.fasta -taxon ./Datasets/taxa2.txt  -marker COI-5p
```

Appendix code 2.The makeblastdb command to create databases from the metadatabases.

```
makeblastdb -in new_sequences.fasta -out Sequences -parse_seqids -dbtype nucl
```

Appendix code 3.The blastn command to query the best matches bettwween our databases and the output from makeblastdb command.

```
blastn -db Sequences -query test.fasta -num_threads 2 -out output.blasted -outfmt
"6 qseqid qlen sseqid slen qstart qend sstart send evalue bitscore
length pident nident mismatch gapopen gaps qseq sseq delim=;";
```

Appendix code 4.The script of mafft to submit on metacentrum to align the obtained COI sequences.

```
#PBS -N MAFFT1_qsub
#PBS -l select=1:ncpus=5:mem=1gb:scratch_local=1gb
#PBS -l walltime=00:59:00

#clean scratch after the end
trap 'clean_scratch' TERM EXIT

# go to  scratch directory
cd $SCRATCHDIR || exit 1

module load mafft

mafft --maxiterate 1000 --globalpair --reorder --thread 5 sequence.fasta > new_alignment/output.fasta
```

Appendix code 5.The script of iqtree2 to submit on Metacentrum to construct the phylogeny tree.

```
#PBS -N IQTREE_qsub
#PBS -l select=1:ncpus=2:mem=1gb:scratch_local=1gb
#PBS -l walltime=00:59:00

#clean scratch after the end
trap 'clean_scratch' TERM EXIT

# go to  scratch directory
cd $SCRATCHDIR || exit 1

source /storage/plzen1/home/trahch00/.bashrc
#module load iqtree

iqtree2 -s output.fasta -p alignment.partitions -B 1000
--boot-trees --wbtl --alrt 1000 --abayes --bnni -m MFP --merge -g alignment.constraints
--date alignment.calibration --prefix ML_calibration --date-tip 0 --date-root -110
--date-outgroup -o "KX781955.1" --date-options "-u 0.1 -l -1" -T 2
```

Appendix code 6. Code to plot the regression plot by family on the Tb depending on Ta.

```r
library(ggplot2)

setwd("../measurement/buffering_ability")

lp <- read.csv("lp_correctfam.csv", encoding = "UTF-8")
lp[lp==""] <- NA
lp[lp=="?"] <- NA
lp <-  na.omit(lp)

# Convert the variables to numeric values

lp$Tbody<-as.numeric(lp$Tbody)
lp$Tair<- as.numeric(lp$Tair)


#store the unique value of family for iterate
family <- as.vector(unique(lp$family))



k_purple <- "#800080"  # Purple color
k_orange <- "#FFA500"  # Orange color

# plot hist for butterfly vs temp air
for (f in family){

 tmp <- subset(lp, lp$family == f)
 air <- tmp$Tair
 body <- tmp$Tbody
 xy.limits <- range( c(air,body) )

 p <- ggplot(data = data.frame(air, body),
         mapping = aes(x = air, y = body)) +
  geom_point(size = 2) +
  scale_color_manual(values = c(k_purple, k_orange)) +
  theme_classic() +
  geom_smooth(method = "lm") +
  ggtitle(f)+
  theme(plot.title = element_text(hjust = 0.5))+
  xlab("Air Temperature (°C)") +
  ylab("Body Temperature (°C)")+
  xlim(c(15,40))+ ylim(15,40)+

  scale_x_continuous(limits=xy.limits) +
  scale_y_continuous(limits=xy.limits) +
  coord_fixed( ratio=1)+
```

```
  theme(
    axis.title.x = element_text(size =20),
    axis.title.y = element_text(size = 20),
    title =  element_text(size = 22),
    legend.text = element_text(size =17),
    axis.text.x = element_text(size =17),
    axis.text.y = element_text(size =17)
  )+
  annotate(
    "text",
    x = mean(range(air)),
    y = min(body),
    label = paste0("Slope == ", round(coef(lm(body ~ air))[2], 3)),
    parse = TRUE,
    size = 7
  )


 # Save the plot with the species name
 plot_filename <- paste0("plots/lines_", f, "_plot.png")
 ggsave(plot_filename, plot = p)
}
```

Appendix code 7. Code to plot the regression lines of each species.

```
library(dplyr)
library(ggplot2)

setwd("C:/Users/anhch/OneDrive/Desktop/Thesis/dataset 2022/R studio/measurement/buffering_ability")

leps1<-read.csv("dataset.csv", fileEncoding = "UTF-8-BOM", sep = ",",row.names=1)

data <- read.csv("species_names.csv", fileEncoding = "UTF-8-BOM")



#data frame of species with no >= 5
leps_edit1 <- leps1 %>%
 dplyr::select(., species_final, Tbody, Tair,family) %>%
 dplyr::count(., species_final) %>%
 dplyr::filter(., species_final %in% data$species_names) %>%
 dplyr::filter(., n >= 5) %>%
 dplyr::filter(., !species_final == ")

#data frame with required data
leps_edit <- leps1 %>%
 dplyr::select(., species_final, Tbody, Tair,family) %>%
 dplyr::filter(., species_final %in% data$species_names, family %in% data$family) %>%
 dplyr::filter(., !species_final == ")
```

```r
#select species from leps_edit that is present in leps_edit1
lp <- leps_edit[as.vector(leps_edit$species_final) %in% (as.vector(leps_edit1$species_final)),]
# drop all the NÁ
lp[lp==""] <- NA
lp[lp=="?"] <- NA
lp <-  na.omit(lp)

# Convert the data into numeric
lp$Tbody<-as.numeric(lp$Tbody)


lp$Tair<- as.numeric(lp$Tair)

# Initiate new values
tab <- list()
mod <- list()
species <- as.vector(unique(lp$species))
# Create empty dataframe

for(i in species)
{
  tab[[i]] <- data.frame(M =NA,  Inter = NA, R2= NA, family = NA)
}


k_purple <- "#800080"  # Purple color
k_orange <- "#FFA500"  # Orange color


# Iterate through the species loop and plot the regression lines for each species
# And store values for the unique species.

for (spec in species) {

  tmp <- subset(lp, lp$species == spec)
  air <- tmp$Tair
  body <- tmp$Tbody
  family <- unique(tmp$family)

  mod_tmp <- lm(body ~ air)
  mod[[spec]] <- mod_tmp
  cf <- coef(mod[[spec]])

  tab[[spec]][1, "M"] <- cf[2]
  tab[[spec]][1, "Inter"] <- cf[1]
  tab[[spec]][1, "R2"] <- summary(mod_tmp)$adj.r.squared
  tab[[spec]][1, "family"] <- family
```

```r
# Create a ggplot and save it as an object
p<- ggplot(data = data.frame(air, body),
        mapping = aes(x = air, y = body)) +
  geom_point(size = 2) +
  scale_color_manual(values = c(k_purple, k_orange)) +
  theme_classic() +
  geom_smooth(method = "lm") +
  ggtitle(spec)+
  theme(plot.title = element_text(hjust = 0.5))+
  xlab("Air Temperature (°C)") +
  ylab("Body Temperature (°C)")+
  annotate("text", x = mean(range(air)), y = min(body),
        label = bquote(italic(Slope(M)) == .(format(cf[2], digits = 3))),
        vjust = 1, hjust = 0.5, color = "black")

 # Save the plot with the species name
plot_filename <- paste0("plots/lines_", spec, "_plot.png")
ggsave(plot_filename, plot = p)
}


# Convert the list into the dataframe

tabs2 <- bind_rows(tab, .id = 'column_label')
```

Appendix code 8. Code to summarize the slopes of each species per family.

```r
# summary of Slope by families

summary_slope_byfamily <- tabs2%>%
 group_by(family) %>%
 summarise(
  Mean_slope = format(round(mean(M, na.rm = TRUE), 2), nsmall =2),
  Min_slope = format(round(min(M, na.rm = TRUE), 2), nsmall =2),
  Max_slope = format(round(max(M, na.rm = TRUE), 2), nsmall =2),
  SD  = format(round(sd(M, na.rm = TRUE), 2), nsmall =2),

 )
```

Appendix code 9. Code to round and calculate the frequency of the Ta and Tb across the families.

```python
import pandas as pd
import matplotlib.pyplot as plt
import math

def round_all(input_file):
    """ function to round all number of body and
air temperature in the dataframe """

    file = pd.read_csv(input_file, index_col=0)
    file= file.dropna()
```

```python
    lst = []

    for values in file.values:
        species = values[0]


        # Convert to numeric with 'coerce' to handle non-numeric values
        Tbody = pd.to_numeric(values[1], errors='coerce')

        # Check for NaN before rounding
        if not pd.isna(Tbody):
            Tbody = math.ceil(Tbody)

        # Convert to numeric with 'coerce' to handle non-numeric values
        Tair = pd.to_numeric(values[2], errors='coerce')

        # Check for NaN before rounding
        if not pd.isna(Tair):
            Tair = math.ceil(Tair)

        family = values[3]

        # Check if 'Tbody' or 'Tair' is of type str and convert it to numeric
        if isinstance(Tbody, str):
            Tbody = pd.to_numeric(Tbody, errors='coerce')
            if not pd.isna(Tbody):
                Tbody = math.ceil(Tbody)

        if isinstance(Tair, str):
            Tair = pd.to_numeric(Tair, errors='coerce')
            if not pd.isna(Tair):
                Tair = math.ceil(Tair)
        lst.append([species, Tbody, Tair, family])

    new_df = pd.DataFrame(lst, columns=['species', 'Tbody', 'Tair', 'family'])
    return new_df

def calculate_freq(input_file, column_name):

    """ Function to count all the number of the
body temperature (Tb) and air temperature (Ta)
appearing within family as well as calculate
the frequency of it (the total number of the Ta
or Tb divided by the total Ta or Tb in that family).

    """
    file = round_all(input_file)

    file[column_name] = pd.to_numeric(file[column_name], errors='coerce')
    file = file.dropna(subset=[column_name])  # Drop rows with NaN or inf in 'Tair' column
    file[column_name] = file[column_name].round().astype(int)
```

```python
    # Group by 'family' and the specified column, then calculate the count
    result = file.groupby(['family', column_name]).size().reset_index(name='count')

    # Calculate the sum of counts for each family
    family_counts = result.groupby('family')['count'].transform('sum')

    # Add a new column for the frequency of each count
    result['frequency'] = (result['count'] / family_counts) * 100

    result.to_csv(f"{column_name}.csv", index=False)

    return result
```

Appendix code 10. Code to plot the histograms for Ta and Tb faceted by families.

```r
library(ggplot2)
library(dplyr)

setwd(".../buffering_ability")

air_data <- read.csv("Tair.csv")
body_data <- read.csv('Tbody.csv')

count_data <- bind_rows(
  mutate(air_data, dataset = "Air temperature"),
  mutate(body_data, dataset = "Body temperature")
)

ggplot(count_data, aes(x = Tair, y = frequency, fill = dataset)) +
  geom_bar(aes(x = Tbody, y = frequency, fill = dataset), stat = "identity", position = "dodge", alpha = 0.7) +  # Adjust alpha for transparency
  geom_bar(stat = "identity", position = "dodge", alpha = 0.7) +  # Adjust alpha for transparency
  facet_wrap(~family, scales = "free_y") +
  labs(title = "Histograms of ambient  temperature and body temperature by family",
x = "Air temperature/ Body temperature", y = "Frequency (%)", fill ='Datasets') + theme_minimal()
```

Appendix code 11. Code to run the comparative analysis PIC and PGLS and plot the ancestral states for the slope on the morphometrics.

```r
library(dplyr)
library(ape)
library(caper)
library(phytools)
library(nlme)

setwd(".../Comparative analysis")

# read data for slopes value
```

```r
tabs2 <- read.csv("tabs2_aircenter.csv", fileEncoding = "UTF-8-BOM")
tabs2 <- tabs2 %>% dplyr:: rename("species" = "column_label")
#new
tabs2$log_M <- log(tabs2$M)


size <- read.csv("Size_qualifications_update_DL.csv", fileEncoding = "UTF-8-BOM")



#new
size$log_wing_loading <- log(size$wing_loading)
size$log_total_area.cm2. <- log(size$total_area.cm2.)
size$log_aspect_ratio <- log(size$aspect_ratio)
size$log_Thorax_Volume <- log(size$Thorax.Cylinder.volume)

tree <- read.tree("final_tree.tre")
#new
rename <- read.table("rename.csv", header=TRUE, sep=",", stringsAsFactors=FALSE, quote="");
tree$tip.label <- rename[[2]][match(tree$tip.label, rename[[1]])];
tree$node.label <- NULL



join_table <- left_join(size, tabs2, by ='species')



write.csv(join_table, file = "slopes_all_table.csv")




# plot slopes against wing_loading

data <- read.csv("slopes_all_table.csv")


trait.X <- (data$log_wing_loading)
names(trait.X) <- data$species
trait.Y <- (data$M)
names(trait.Y) <- data$species



par(mfrow=c(4,2))
#PIC
pic.trait.Y <- pic(trait.Y, tree)
pic.trait.X <- pic(trait.X, tree)

summary(pic.trait.Y)
summary(pic.trait.X)

plot(pic.trait.X, pic.trait.Y, xlab ="pic_Wing_Loading (log)",xlim = c(-0.2, 0.3), ylim= c(-0.15, 0.1),
ylab=  "pic_Buffering ability (Slopes)")
```

```r
fit.lm.pic <- lm(pic.trait.Y ~ pic.trait.X - 1) # we fit the lm without1 an intercept term
abline(fit.lm.pic, col = "red")
summary(fit.lm.pic)

#new PGLS
brownian = corBrownian(value = 1, tree, form=~species)
pgls = gls(M ~ log_wing_loading, data = data, correlation = brownian, method="ML")
summary(pgls)
plot(trait.X, trait.Y, xlab ="Wing Loading (log)", ylab= "Buffering ability (Slopes)")
abline(a = coef(pgls)[1], b = coef(pgls)[2], col = "red")

slope_wingloading <- coef(lm(pic.trait.Y ~ pic.trait.X -1))

# plot slopes with total area

trait.X <- (data$log_total_area.cm2.)
names(trait.X) <- data$species


#PIC
pic.trait.X <- pic(trait.X, tree)

plot(pic.trait.X , pic.trait.Y, xlab = "pic_log Total Area (cm2)", ylab = "pic_Buffering ability (Slopes)")
fit.pic.MT = lm(pic.trait.Y ~ pic.trait.X -1)
abline(fit.pic.MT, col = "red")
summary(fit.pic.MT)

#new PGLS
pgls = gls(M ~ log_total_area.cm2., data = data, correlation = brownian, method="ML")
summary(pgls)
plot(trait.X, trait.Y, xlab ="log Total Area (cm2)", ylab= "Buffering ability (Slopes)")
abline(a = coef(pgls)[1], b = coef(pgls)[2], col = "red")



slope_area <- coef(lm(pic.trait.Y ~ pic.trait.X -1))




# plot slopes with aspect ratio

trait.X <- data$aspect_ratio
names(trait.X) <- data$species

#PIC
pic.trait.X <- pic(trait.X, tree)

plot(pic.trait.X , pic.trait.Y, xlab = "pic_aspect_ratio", ylab = "pic_Buffering ability (Slopes)")
fit.pic.MT = lm(pic.trait.Y ~ pic.trait.X -1)
abline(fit.pic.MT, col = "red")
```

```r
summary(fit.pic.MT)

#new PGLS
pgls = gls(M ~ aspect_ratio, data = data, correlation = brownian, method="ML")
summary(pgls)
plot(trait.X, trait.Y, xlab ="Aspect ratio", ylab= "Buffering ability (Slopes)")
abline(a = coef(pgls)[1], b = coef(pgls)[2], col = "red")

slope_aspectratio <- coef(lm(pic.trait.Y ~ pic.trait.X -1))
slope_aspectratio

# plot slopes with thorax volume

trait.X <- data$log_Thorax_Volume
names(trait.X) <- data$species

#PIC
pic.trait.X <- pic(trait.X, tree)



plot(pic.trait.X , pic.trait.Y, xlab = "pic_Thorax_volume (log)", ylab = "pic_Buffering ability (Slopes)")
fit.pic.MT = lm(pic.trait.Y ~ pic.trait.X -1)
abline(fit.pic.MT, col = "red")
summary(fit.pic.MT)

#new PGLS
pgls = gls(M ~ log_Thorax_Volume, data = data, correlation = brownian, method="ML")
summary(pgls)
plot(trait.X, trait.Y, xlab ="Thorax Volume (log)", ylab= "Buffering ability (Slopes)")
abline(a = coef(pgls)[1], b = coef(pgls)[2], col = "red")



slope_thoraxvolume <- coef(lm(pic.trait.Y ~ pic.trait.X -1))



#new plot ancestral states
par(mfrow=c(1,1))
#new plot ancestral states
# Slopes
obj.M <- contMap(tree, trait.Y);
# Wing_loading
trait.WL <- (data$log_wing_loading)
names(trait.WL) <- data$species
obj.WL <- contMap(tree, trait.WL);
#Total Area
trait.TA <- (data$log_total_area.cm2.)
names(trait.TA) <- data$species
obj.TA <- contMap(tree, trait.TA);
# Aspect Ratio
```

```r
trait.AR <- (data$aspect_ratio)
names(trait.AR) <- data$species
obj.AR <- contMap(tree, trait.AR);
# Thorax Volume
trait.TV <- data$log_Thorax_Volume
names(trait.TV) <- data$species
obj.TV <- contMap(tree, trait.TV);


plot(obj.M, ylim=c(1-0.09*(Ntip(obj.M$tree)-1), Ntip(obj.M$tree)), mar=c(0.5,0.5,2,0.5))
title("Buffering ability (Slopes)")

plot(obj.WL, ylim=c(1-0.09*(Ntip(obj.WL$tree)-1), Ntip(obj.WL$tree)), mar=c(0.5,0.5,2,0.5))
title("Wing Loading (log)")

plot(obj.TA, ylim=c(1-0.09*(Ntip(obj.TA$tree)-1), Ntip(obj.TA$tree)), mar=c(0.5,0.5,2,0.5))
title("Total Area (log)")

plot(obj.AR, ylim=c(1-0.09*(Ntip(obj.AR$tree)-1), Ntip(obj.AR$tree)), mar=c(0.5,0.5,2,0.5))
title("Aspect Ratio")

plot(obj.TV, ylim=c(1-0.09*(Ntip(obj.TV$tree)-1), Ntip(obj.TV$tree)), mar=c(0.5,0.5,2,0.5))
title("Thorax Volume (log) ")
```